การสังเคราะห์อนุภาคเงินที่ควบคุมขนาดได้ด้วยเคมีที่เป็นมิตรกับสิ่งแวดล้อม

นางสาววิมลนันท์ สร้อยสุริยา

วิทยานิพนธ์นี้เป็นส่วนหนึ่งของการศึกษาตามหลักสูตรปริญญาวิทยาศาสตรดุษฎีบัณฑิต
สาขาวิชาเคมี ภาควิชาเคมี
คณะวิทยาศาสตร์ จุฬาลงกรณ์มหาวิทยาลัย
ปีการศึกษา 2554

SIZE-CONTROLLED SYNTHESIS OF SILVER PARTICLES
VIA GREEN CHEMISTRY

Miss Wimonnan Sroisuriya

A Dissertation Submitted in Partial Fulfillment of the Requirements
for the Degree of Doctor of Philosophy Program in Chemistry
Department of Chemistry
Faculty of Science
Chulalongkorn University
Academic Year 2011

Thesis Title   SIZE-CONTROLLED SYNTHESIS OF SILVER PARTICLES VIA GREEN CHEMISTRY

By   Miss Wimonnan Sroisuriya

Field of Study   Chemistry

Thesis Advisor   Associate Professor Sanong Ekgasit, Ph.D.

Thesis Co-advisor   Associate Professor Chuchaat Thammacharoen

---

        Accepted by the Faculty of Science, Chulalongkorn University in Partial Fulfillment of the Requirements for the Doctoral Degree

………………………………………Dean of the Faculty of Science

(Professor Supot Hannongbua, Dr.rer.nat.)

THESIS COMMITTEE

………………………………………Chairman

(Assistant Professor Warinthorn Chavasiri, Ph.D.)

………………………………………Thesis Advisor

(Associate Professor Sanong Ekgasit, Ph.D.)

………………………………………Thesis Co-advisor

(Associate Professor Chuchaat Thammacharoen)

……………………………………….Examiner

(Associate Professor Vithaya Ruangpornvisuti, Dr.rer.nat.)

……………………………………….External Examiner

(Associate Professor Vittaya Amornkitbamrung, Ph.D.)

วิมลนันท์ สร้อยสุริยา : การสังเคราะห์อนุภาคเงินที่ควบคุมขนาดได้ด้วยเคมีที่เป็นมิตรกับสิ่งแวดล้อม. (SIZE-CONTROLLED SYNTHESIS OF SILVER PARTICLES *VIA* GREEN CHEMISTRY) อ.ที่ปรึกษาวิทยานิพนธ์หลัก: รศ.ดร.สนอง เอกสิทธิ์, อ.ที่ปรึกษาวิทยานิพนธ์ร่วม: รศ. ชูชาติ ธรรมเจริญ, 64 หน้า.

อนุภาคระดับนาโนเมตรของเงินประสบความสำเร็จในการสังเคราะห์ด้วยเคมีที่เป็นมิตรกับสิ่งแวดล้อม โดยใช้แป้งมันทำหน้าที่เป็นตัวรีดิวซ์และสารช่วยเสถียร หลังจากปรับสภาพแป้งมันโดยการไฮโดรไลซิสด้วยกรดและสลายแป้งมันด้วยด่าง แป้งมันสามารถให้รีดิวซิ่งสปีชีส์ สามารถรีดิวซ์ไอออนของโลหะเงินได้สมบูรณ์และช่วยรักษาเสถียรภาพของอนุภาคระดับนาโนเมตรของเงิน การวิเคราะห์ขนาดเฉลี่ย การกระจายตัวของอนุภาค ลักษณะรูปร่างและโครงสร้างของอนุภาคระดับนาโนเมตรของเงินที่สังเคราะห์ได้ โดยใช้เทคนิคยูวี-วิสิเบิล สเปกโทรสโกปี กล้องจุลทรรศน์อิเล็กตรอนชนิดส่องผ่านและเอกซ์เรย์ดิฟแฟรกชัน พบว่าอนุภาคระดับนาโนเมตรของเงินที่สังเคราะห์ได้เกิดเซอร์เฟสพลาสมอนเรโซแนนซ์พีคที่ประมาณ 400 นาโนเมตร อนุภาคมีลักษณะทรงกลม ขนาดเฉลี่ยประมาณ 15 ± 2.3 นาโนเมตร และมีการกระจายตัวของขนาดที่แคบ ผลจากเอกซ์เรย์ดิฟแฟรกชัน พบว่าอนุภาคระดับนาโนเมตรของเงินมีโครงสร้างผลึกเป็นลูกบาศก์แบบเฟสเซ็นเตอร์ การสลายของแป้งมันโดยใช้กรดและด่างวิเคราะห์โดยใช้เทคนิคเอทีอาร์ ฟูเรียทรานส์ฟอร์ม อินฟราเรดสเปกโทรสโกปี อนุภาคระดับนาโนเมตรของเงินที่สังเคราะห์ได้มีเสถียรภาพดีเมื่อเก็บไว้ที่อุณหภูมิห้องอย่างน้อยที่สุด 2 เดือน โดยไม่ตกตะกอน สมบัติด้านการยับยั้งเชื้อแบคทีเรียของอนุภาคเงินระดับนาโนเมตรที่มีต่อ *Staphylococcus aureus* และ *Escherichia coli* พบว่าความเข้มข้นต่ำสุดของอนุภาคระดับนาโนเมตรของเงินเท่ากับ 2.5 ppm สามารถยับยั้งเชื้อแบคทีเรียได้

ภาควิชา .... เคมี .... ลายมือชื่อนิสิต ....

สาขาวิชา .... เคมี .... ลายมือชื่อ อ.ที่ปรึกษาวิทยานิพนธ์หลัก ....

ปีการศึกษา .... 2554 .... ลายมือชื่ออ.ที่ปรึกษาวิทยานิพนธ์ร่วม ....

5073879823 : MAJOR   CHEMISTRY

KEYWORDS : GREEN SYNTHESIS/SILVER NANOPARTICLES/TAPIOCA/ ALKALINE DEGRADATION/ANTIBACTERIAL ACTIVITY

WIMONNAN SROISURIYA: SIZE-CONTROLLED SYNTHESIS OF SILVER PARTICLES VIA GREEN CHEMISTRY. ADVISOR: ASSOC. PROF. SANONG EKGASIT, PH.D., CO-ADVISOR: ASSOC. PROF. CHUCHAAT THAMMACHAROEN, 64 pp.

Silver nanoparticles (AgNPs) were successfully synthesized using "green chemistry". Tapioca has been used both as reducing agent and stabilizer. Tapioca after treated with an acidic and alkaline solution generated reducing species which is used to completely reduce silver ions and sufficiently stabilize the obtained silver nanoparticles. The average size, size distribution, morphology, and structure of the synthesized silver nanoparticles were characterized by Ultraviolet-visible spectroscopy (UV-vis), transmission electron microscopy (TEM), and X-ray diffraction (XRD). Strong surface plasmon resonance peaks were observed at about 400 nm and the synthesized silver nanoparticles were spherical with an average particle size of 15 ± 2.3 nm with a narrow particle size distribution. XRD analysis showed that the silver nanoparticles were face centered cubic (fcc) structure. The degradation of tapioca *via* an acidic and alkaline treatment was investigated by ATR FT-IR spectroscopy. The synthesized silver nanoparticles are stable in aqueous solution over a period of two months at room temperature. The antibacterial activities of the silver nanoparticles were tested against *Staphylococcus aureus* and *Escherichia coli* bacteria. A very low concentration of silver nanoparticles (2.5 ppm) was shown to be an effective bactericide.

Department : _____Chemistry_____   Student's Signature _____

Field of Study : _____Chemistry_____   Advisor's Signature _____

Academic Year :____2011_____   Co-advisor's Signature _____

ACKNOWLEDGEMENTS

I would like to express my sincere gratitude to my thesis advisor, Associate Professor Dr. Sanong Ekgasit and my thesis co-advisor Associate Professor Chuchaat Thammacharoen for wholeheartedly provide the useful guidance, understanding, training and teaching the theoretical background and technical skills during my research.

I would like to thank Assistant Professor Dr. Warinthorn Chavasiri, Associate Professor Dr. Vithaya Ruangpornvisuti, and Associate Professor Dr.Vittaya Amornkitbamrung for usefully substantial suggestions as the thesis committee.

I would like to thank the Commission on Higher Education (CHE) for supporting grant under the Program Strategic Scholarships for Frontier Research Network for the Ph. D. Program Thai Doctoral degree for this research.

Partial financial support from National Center of Excellence for Petroleum, Petrochemical and Advanced Materials (CE-PPAM).

Warmest thanks to my friends, my colleagues and organization: Sensor Research Unit, Department of Chemistry, Faculty of Science, Chulalongkorn University, and all good friends for the suggestions and spiritual supports throughout this research.

Whatever shortcomings in the thesis remain, they are the sole responsibility of the author.

Above all, I would like to express my special gratitude to my parents, family members for their inspiration, understanding, great support and encouragement throughout the entire course of study.

CONTENTS

LIST OF TABLES

LIST OF FIGURES

LIST OF SCHEMES

LIST OF ABBREVIATIONS

AgNO$_3$: silver nitrate

AgNPs   : silver nanoparticles

NaBH$_4$: sodium borohydride

LSPR   : localized surface plasmon resonance

nm   : nanometer

Ag   : Argentum (silver)

ppm   : part per million

M   : molar

g   : gram

°C   : degree Celsius

PVP   : polyvinylpyrrolidone

TEM   : transmission electron microscopy

XRD   : x-ray diffraction

ATR FT-IR   : attenuated total reflection Fourier transform infrared

UV-vis   : ultraviolet-visible spectroscopy

FWHM   : full width at half maxima

CFU   : coloni-forming unit

IRE   : internal reflection element

CHAPTER I

INTRODUCTION

1.1 Synthesis of silver nanoparticles

The large surface area and small size of nanoparticles provide the unique chemical, optical, mechanical, electronic and magnetic properties that are distinct from those bulk materials. These unique properties are derived due to several variations such as size distribution and structure of particles. Therefore, nanoparticles have received considerable attention and rapidly growth in the recent year with wide ranging implications in a variety of areas such as drug delivery, colorimetric sensors, diagnostics and antibacterial [1-9]. The broad applications of silver nanoparticles (AgNPs) encourage the high demanding of industries for adding them into the consumer products. There are several conventional synthesis protocols which involves the number of chemical and physical methods. Physical fabrication methods of metal nanoparticles employ inert gas condensation [10], laser ablation [11], spray pyrolysis 12-13], radiation [14], and thermal plasma [15]. However, the methods are high energy consumption, expensive, employ toxic chemicals, and often give low yields. The chemical route to synthesize AgNPs involves the reduction of silver ion by reducing agents such as sodium borohydride [16], trisodium citrate [17-18], hydroxylamine hydrochloride [17], alcohol and glucose [19]. In order to prevent the aggregation of metal particles, surface protecting agent is necessary. Usually, the common protecting agents are sodium citrate, poly (vinyl pyrrolidone) [20], polyacrylate [21], and poly (vinyl alcohol) [22].

Nowadays, many researches preferred an environmental-friendly method for synthesizing AgNPs than the conventional methods involving hazardous chemicals. Green chemistry principles which involve a reduction or elimination of the use of generation of hazardous substances, play an important role in nanotechnology research. Three areas of opportunity to associate metal nanoparticles synthesis with

green chemistry principle: (1) choice of solvent, (2) the reducing agent, and (3) the dispersing agent [23]. The environmental friendly reducing agents, for instance, β-D-glucose [5, 24], galactose [24], maltose [24], lactose [24], L-lysine [25], L-arginine [25], soluble starch [5, 26-28], latex of *Jatopha curcas* [30], fish oil [31] , and banana peel extract [32] have been used to synthesize AgNPs.

In this work, we developed green chemical method to synthesize silver nanoparticles using tapioca as an efficient reducing agent and stabilizer. Tapioca is agricultural product and largely cultivated. It is inexpensive and available in local market. In addition, it is non-toxic compared to other reducing agents. Synthesis of silver nanoparticles using tapioca, is accordance with the green chemistry principles: the tapioca is (1) eco-friendly as well as (2) the reducing employed, and (3) the stabilizer in the reaction. The results showed that the tapioca after treated with an acidic and alkaline solution generated reducing species which is used to reduce silver ion into silver nanoparticles.

1.2 The objectives of the research

1. To develop new synthesis route of silver nanoparticles via green chemistry.
2. To investigate the suitable conditions for preparations of silver nanoparticles which well-defined size by using tapioca as both reducing agent and stabilizer.

1.3 Scopes of the research

1. Study the effect of amount of sodium hydroxide, concentration of silver nitrate, concentration of tapioca, reaction temperature on size, size distribution and morphology of synthesized silver nanoparticles.
2. Characterize size, size distribution, morphology, and structure of synthesized silver nanoparticles using UV-visible spectroscopy, transmission electron microscopy (TEM), and X-ray diffraction (XRD).
3. Investigating the degradation of tapioca under an acidic and alkaline treatment by ATR FT-IR spectroscopy.

4. Study the stability of synthesized silver nanoparticles.

5. Comparison of green synthesis method and conventional method (sodium borohydride method).

6. Investigating the antibacterial property of synthesized silver nanoparticles against the gram-negative bacterium *Escherichia coli (E. coli)* and gram-positive bacterium *Staphylococcus aureus (S. aureus).*

CHAPTER II

THEORETICAL BACKGROUND

2.1 Silver nanoparticles

Silver nanoparticles are of great interests in scientific research and industrial applications, due to the large surface area to volume ratio and size-dependent properties. Silver nanoparticles have been used in different areas of science such as catalysis [15-16], surface enhance vibration [17], optical sensor [22, 25, 28-29], and antibacterial agent [2-7].

Noble metal nanoparticles (especially gold and silver) exhibit a strong UV-visible absorption band that is not present in the spectrum of the bulk metal. This absorption band is observed when the incident photon frequency is resonant with the collective oscillation of the conduction electrons and is known as the localized surface plasmon resonance (LSPR) [1]. When the environment of metal nanoparticles was changed, LSPR shifts were observed. Electromagnetic field enhancement near the surface of nanoparticles is associated with extinction efficiency of nanoparticles, responsible for the intense signals.

The developments of synthesis methods for silver nanoparticles have been explored in order to control size and shape of particles [20-21]. There are many methods to synthesize silver nanoparticles. In general, the synthesis methods are classified into two categories, "bottom-up" and "top-down" approaches. Bottom-up approach is getting started with the atom or molecule for building up the desired nano-objects. In contrast to top-down approach, standard bulk material are broken down and produced the same materials in the form of nanometric grains.

2.2 Conventional methods for synthesis of silver nanoparticles

There are several conventional synthesis protocols which involves a number of physical and chemical methods. Physical fabrication methods of metal nanoparticles employ inert gas condensation [10], laser ablation [11], spray pyrolysis [12-13], gamma ray [14], and thermal plasma [15]. However, the methods are high energy consumption, expensive, employ toxic chemicals, and often give low yields. The synthetic route to synthesize AgNPs involves the reduction of Ag ion by reducing agents such as sodium borohydride [16], trisodium citrate [17-18], hydroxylamine hydrochloride [17], alcohol and glucose [19]. In order to prevent the aggregation of metal particles, surface protecting agent is necessary. Usually, the common protecting agents are sodium citrate, poly (vinyl pyrrolidone) [20], polyacrylate [21], and poly (vinyl alcohol) [22]. The reviews express the concern with the synthesis of silver nanoparticles by using extreme conditions (e.g., high pressure, high temperature), hazardous reagent, organic solvent, and stabilizer. Presently, many researches tend to make environmental friendly method, green chemistry to design the reaction or choose the environmental benign for synthesis of silver nanoparticles.

2.3 Synthesis of silver nanoparticles *via* green chemistry

Nowadays, many researches preferred an environmentally-friendly method for synthesizing AgNPs to the conventional method involving hazardous chemicals. Green chemistry principles which involve a reduction or elimination of the use of generation of hazardous substances, play an important role in nanotechnology research.

2.3.1 Green chemistry principle

Green chemistry is "the utilization of a set of principles that reduces or eliminates the use or generation of hazardous substances in the design, manufacture, and application of chemical products" [23]. The 12 principles of green chemistry are summarized in Table 2.1. Application of these principles has reduced the use of toxic

chemical and solvents, improved the material and energy efficiency of chemical processes, and enhanced the design of products for end of life.

Table 2.1 12 green chemistry principles [23].

Principles of green chemistry	Design to greener nanomaterial and production method
P1. Waste prevention	design to prevent waste than to treat or clean up waste after it has been created
P2. Atom economy	design to maximize all of the materials use in the synthetic process to final product
P3. Less hazardous chemical synthesis	design to a little use or generate the hazardous substance
P4. Designing safer chemicals	design the desire product with minimizing their toxicity
P5. Safer solvents/reaction media	design to make a necessary use of substances (e.g., solvents)
P6. Design for energy efficiency	design to minimize energy using.
P7. Use of renewable feed stocks	design to used renewable raw material or feedstock
P8. Reduce derivatives	design to minimize or avoid the using of unnecessary derivative (e.g., protection
P9. Catalysis	design to use the catalytic reagent which as selective as possible
P10. Design for degradation/ design for end of life	design to gain the product which non-toxic and environmentally benign
P11. Real-time monitoring and process control	design to develop the real-time analysis for prevention of the formation of hazardous substances
P12. Inherently safer chemistry	design to use the potential substance for minimizing of an accident

2.3.2 Literature reviews

The preparation of stable and well-defined shape with controllable size of silver nanoparticles with green synthesis method, the polysaccharide (i.e., starch, carbohydrate, and cellulose base material) is a renewable reagent which widely used as a stabilizer or protecting agent. For example, a starch was used as a stabilizer for synthesis of silver nanoparticles published in a few reports. In 2003 Raveendran et al. [26] reported a completely green synthesis of silver nanoparticles with size of 1-8 nm

using starch as stabilizer and β–D-glucose as reducing agent under gentle heating at 40 °C for 20 hours. This method is limited in long time reaction. There are few works which reported in literature on the green synthesis of silver nanoparticles using soluble starch as both the reducing agent and stabilizer. In 2006 Vigneshwaran et al. [27] synthesized silver nanoparticles using soluble starch as both the reducing and stabilizing agent. This reaction was carried out in an autoclave at 15 psi, 121 °C for 5 minutes. The size of these nanoparticles was found to be in the range of 10-34 nm. The environmental friendly reducing agents, for instance, β-D-glucose [5,24], galactose [25], maltose [25], lactose [25], L-lysine [26], L-arginine [26], soluble starch [5, 27-29], latex of *Jatopha curcas* [30], fish oil [31] , banana peel extract [32], sucrose [33], *Capsicum annuum* L. extract. [34], plant leaf extracts [35], honey [36], tansy fruit [37], *Cyas* Leaf. [38], sorghum bran extracts [39], Murraya Koenigii leaf [40], *Aspergillus flavus* NJP08 [41], chitosan [55], tea extract [7], garlic clove extract [6] are summarized in Table 2.2.

Table 2.2 Literature reviews.
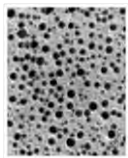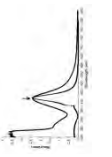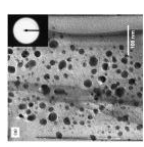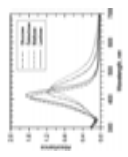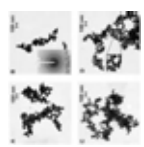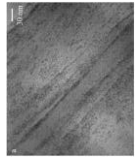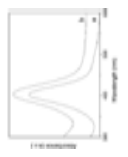
Author/Year	Silver precursor	Reducing agent/ Stabilizer	Condition	UV-vis	TEM	Stability/ Application
Raveendran, P. et al. [26] (2003)	$AgNO_3$	β-D-glucose/ Soluble starch	Heat 40 °C 20 h	λ_{max} 419 nm	1-8 nm	2 months
Vigneshwaran, N. et al. [27] (2006)	$AgNO_3$	Soluble starch	Autoclave 15 psi, 121 °C 5 min	λ_{max} 420 nm	23 nm	3 months
Panacek, A. et al. [5] (2006)	$[Ag(NH_3)_2]^+$	Glucose, Galactose, Lactose, Maltose	Room Temp. Several minutes	λ_{max} 390–420 nm	25-50 nm	-
Manno, D. et al. [28] (2008)	$AgNO_3$	β-D-glucose/ Soluble starch	Boiled 60 min	Broad peak 400-500 nm	1-25 nm	Several months/ hydrogen peroxide sensor
Hu, Y. et al. [16] (2008)	$AgNO_3$	L-lysine, L-arginine/ Soluble starch	Microwave 150 °C 10 s	λ_{max} 403 nm	26 nm	2 months

Table 2.2 Literature reviews (continued).
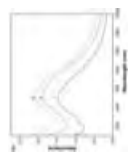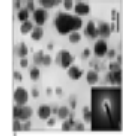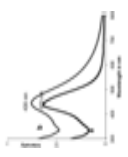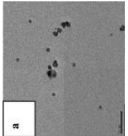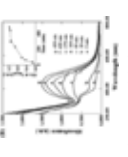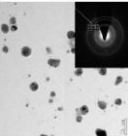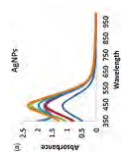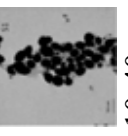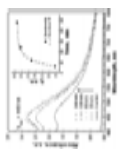
Author/Year	Silver precursor	Reducing agent/ Stabilizer	Condition	UV-vis	TEM	Stability/ Application
Bar, H. et al. [30] (2009)	AgNO$_3$	*Jatropha curcas* latex	Heat 85 °C 4 h	λ_{max} 425 nm	20-30 nm	-
Khanna, P. K. et al. [31] (2009)	AgNO$_3$	Cod liver oil (fish oil)	Heat 120 °C 4 h	λ_{max} 436 nm	5-10 nm	-
Song, J. Y. et al. [35] (2009)	AgNO$_3$	Plant leaf extract (*Magnolia kobus*)	Heat 95 °C 10 min	λ_{max} 430 nm	15 nm	-
Dubey, S. P. et al. [37] (2010)	AgNO$_3$	*Tanacetum vulgare* extract	Room temp. 10 min	λ_{max} 452 nm	10-40 nm	-
Jha, A. K. et al. [38] (2010)	AgNO$_3$	*Cyas* leaf	Steam bath 10 min Incubate 4 hr	λ_{max} 449 nm	2-6 nm	-

Table 2.2 Literature reviews (continued).
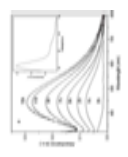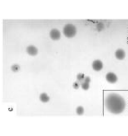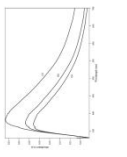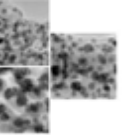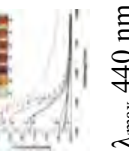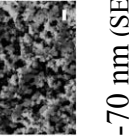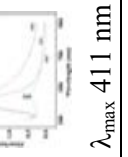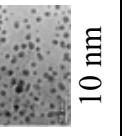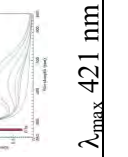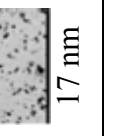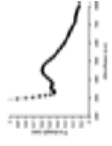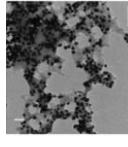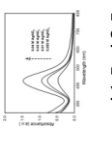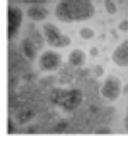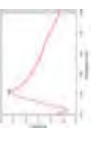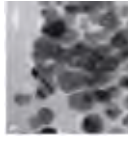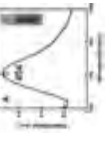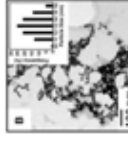
Author/Year	Silver precursor	Reducing agent/ Stabilizer	Condition	UV-vis	TEM	Stability/ Application
Li, S. et al. [34] (2007)	AgNO$_3$	*Capsicum annuum L.* extract	Room Temp. 15 h	λ_{max} 440 nm	30-70 nm	-
Njagi, E. C. et al. [39] (2010)	AgNO$_3$	Sorghum Bran extract	Room Temp. 1 h	λ_{max} 390 nm	10 nm	-
Banker, A. et al. [32] (2010)	AgNO$_3$	Banana peel extract	Adjust pH 3 80 °C 3 min	λ_{max} 440 nm	30-70 nm (SEM)	-
Philip, D. et al. [40] (2011)	AgNO$_3$	Murraya Koenigii leaf extract	Room Temp. 10 min	λ_{max} 411 nm	10 nm	2 months
Jain, N. et al. [41] (2010)	AgNO$_3$	Filtrate of *Aspergillus flavous* NJP08	Incubated at 28 °C, 72 h	λ_{max} 421 nm	17 nm	4 months

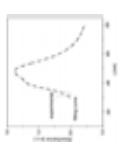**Table 2.2** Literature reviews (continued).

Author/Year	Silver precursor	Reducing agent/ Stabilizer	Condition	UV-vis	TEM	Stability/ Application
Wei, D. et al. [55] (2009)	AgNO$_3$	Chitosan	Heat 95 °C 12 hr	λ_{max} 420 nm	50 nm	Antimicrobial activities (*E. coli*)
Mouton, M. C. et al. [7] (2010)	AgNO$_3$	Tea extract	10:1 ratio of water to tea extract Room Temp.	λ_{max} 450 nm	50 nm	*in vitro* studies (Human keratinocyte cell, HaCaT)
Huang, N. M. et al. [4] (2010)	AgNO$_3$	Sucrose/ dimethyl formamide (DMF)	Heat 30 °C 30 min	λ_{max} 415–425 nm	10 nm	6 month/ antimicrobial activities (*S. aureus*, *A. hydrophila*)
Ahamed, M. et al. [6] (2011)	AgNO$_3$	Garlic clove extract	Heat 50-60 °C 30 min	λ_{max} 408 nm	12 nm	*in vitro* studies (Human lung epithelial A549 cells)
Venkatpurwar, V. et al. [70] (2011)	AgNO$_3$	Sulfated polysaccharide (marine red algae)	Adjust pH 11 Heat 70 °C 15 min	λ_{max} 404 nm	13 nm	6 month/ antimicrobial activities (*S. aureus*, *E. coli*)

2.4 Tapioca

Tapioca is one of largely cultivated agricultural products of Thailand. It is inexpensive and available in local market. Tapioca is a white powder and the chemical structure like a starch (as shown in Figure 2.1). Starch occurs in the form of tiny white granule in various sites of plants, for example in roots (tapioca, sweet potato, yam), in tubers (potatos), in stems (sagopallm), in cereal grains (maize, rice, wheat, barley, oat, sorghum), and in legume seeds (peas, beans) [42].

Figure 2.1 Tapioca

Starches are polysaccharides, composed of a number of monosaccharides or glucose molecules linked together with α-1,4 and/or α-1,6 linkages. The starch consists of 2 main polymers; the amylose, which is a linear glucose polymer with α-1,4 linkages and amylopectin, which is a large branched molecule with α-1,4 and α-1,6 linkages and is a major component of starch [43]. The chemical structure of starch is shown in Figure 2.2.
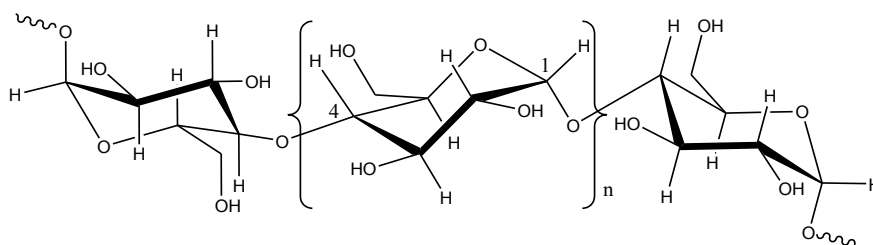
Figure 2.2 The chemical structure of starch [44].

The amylose and amylopectin composition of starch is depending on the plant, starch generally contains 20-25% amylose and 75-80% amylopectin. Tapioca consists of 17% amylose and 83% amylopectin. The percentage of amylose and amylopectin are shown in Table 2.3.

Table 2.3 Amylose and amylopectin in some starches [43].

Starch	Amylose (%)	Amylopectin (%)
Tapioca	17	83
Potato	21	79
Wheat	26	74
Maize	28	72

It has been reported that the reducing end group (aldehyde and α-hydroxy ketone) can be obtained from the degradation of polysaccharide under alkaline condition [64–66]. Soluble starch is polysaccharide which forms a linear polymer by the α-(1$\rightarrow$4) linkages between D-glucose units (Figure 2.2) which can be generated the reducing end group under alkaline degradation. Moreover, the hydroxyl rich on the starch structure can provide the complexation of metal ion to prevent the aggregation or precipitation of metal particles [26-27]. Although, the soluble starch have been served for synthesis and stabilization of AgNPs, however, the reaction is carried out in strong condition, which involves high pressure (15 psi) and high temperature (121°C). In addition, the clarification of reduction reaction mechanism for using degraded products of tapioca under alkaline condition serving as a reducing agent for the metal reduction has not been reported.

In this work, we synthesized silver nanoparticles using tapioca as an efficient reducing agent and stabilizer. Tapioca is agricultural product that largely cultivated. It is inexpensive and available in local market. In addition, no toxicity, compared to other reducing agents. Synthesis silver nanoparticles using tapioca, is compatible with the green chemistry principles: the tapioca is (1) eco-friendly as well as (2) the reducing employed, and (3) the stabilizer in the reaction.

2.5 Characterization techniques

2.5.1 Ultraviolet-visible spectroscopy (UV-vis)

UV-visible spectroscopy is widely used to determine the optical properties of material in solution phase. The absorption in the UV-visible range directly affects the color of material. In case of metal nanoparticles, the optical properties are much more complicated. The measured absorbance spectrum is the extinction of the light, which is the summation of absorption and scattering intensity. Extinction and absorption intensity of spherical particles of arbitrary size can be calculated by Mie's theory [45-48].
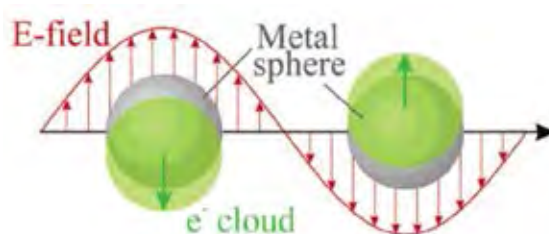
Figure 2.3 LSPR schematic illustration [46].

When the incident photon frequency resonates with the collective oscillation of the conduction electron in the metal nanoparticles is frequency known as a **Localized Surface Plasmon Resonance (LSPR)**. This is schematically pictured Figure 2.3. When the electron cloud is displaced relative to the nuclei, a restoring force arises from Coulomb attraction between electrons and nuclei that results in oscillation of the electron cloud relative to the nuclear framework. The oscillation frequency is determined by four factors: (i) the density of electrons, (ii) the effective electron mass, (iii) the shape and (iv) size of the charge distribution. The collective oscillation of the electrons is called the dipole plasmon resonance of the particle to distinguish from plasmon excitation that can occur in bulk metal or metal surfaces. Higher modes of plasmon excitation can occur, such as the quadrupole mode where half of the electron cloud moves parallel to the applied field and half moves antiparallel. For silver, the plasmon frequency is also influenced by other electrons such as those in d-orbitals, and this prevents the plasmon frequency from being easily calculated using electronic

structure calculations. However, it is not hard to relate the plasmon frequency to the metal dielectric constant, which is a property that can be measured as a function of wavelength for bulk metal.
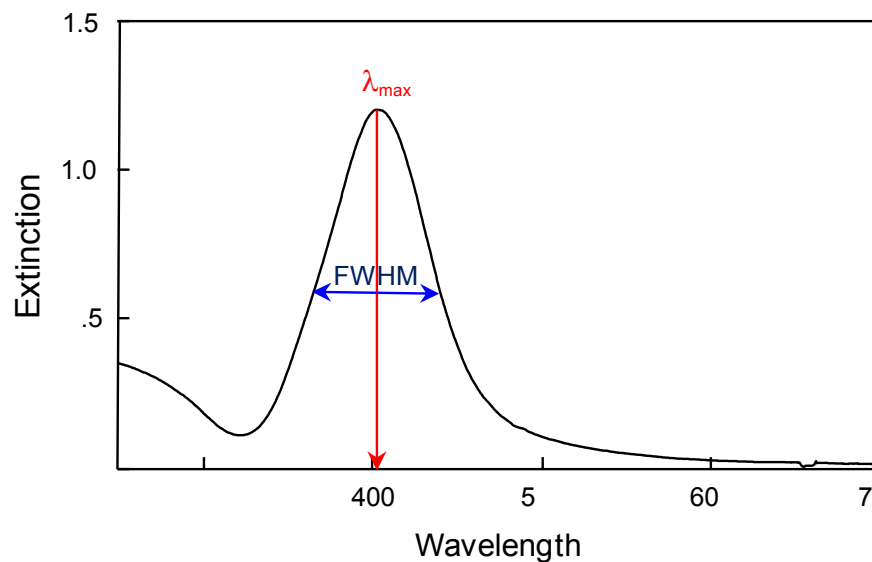
Figure 2.4 The plasmon extinction spectrum of silver nanoparticles.

The particles shape, dimension, and particle size distribution are associated with the measured extinction spectra (Figure 2.4). Therefore, we can obtained the direct particle information from the simple measurement, instead of the complex sample preparation and time-consuming TEM measurement for numerous sample measurements.

2.5.2 Transmission electron microscopy (TEM)

TEM was widely used for studying the size, size distribution, and morphology of particles. TEM involves a beam of accelerated electron with energy of 50-200 keV emitted by a cathode in vacuum. These electrons are deflected in small angles by atoms in sample and transmitted through thin sample. Then, these electrons are magnified by magnetic lenses and hitting a fluorescent screen generating the bright field image. The interactions of electron beam with atoms in the samples are the diffraction or absorption of electron beam. The images from electron microscopes

indicate the morphology of a sample which can be used for determining size and morphology of metal nanoparticles.

2.5.3 Attenuated Total Reflection Fourier Transform Infrared spectroscopy (ATR FT-IR spectroscopy)

ATR FT-IR spectroscopy is the characterization technique based on an internal reflection phenomenon. The radiation travels in a higher refractive index material impinges on the interface with a less dense medium. When incident angle is greater than critical angle, the incident radiation is completely reflected. In addition, there is an electromagnetic field that extends beyond the crystal surface, it is called evanescent wave. If an absorbing material is contacted with internal reflection element (IRE), the evanescent wave will absorb at wavelength where the material has an absorption band. The amount of energy reflected back through the IRE will be attenuated. This technique is called Attenuated Total Reflection.

For ATR technique, the reflectivity is a measurement of the interaction of the electric field with the material. The molecular information and chemical composition can be obtained.

2.5.4 X-ray diffraction (XRD)

The X-ray technique employs the powder diffraction in which the monochromatic beam is incident at an angle θ on a specimen of about 10 mm^2 in area and (for polycrystalline or powder specimens) a minimum thickness of about 20 μm, mounted on a support film that does not give rise to interfering reflections. The detector is set to receive reflections at an angle (the Bragg-Brentano symmetrical arrangement and this is varied over the angular range of interest (typically 1-6° for low-angle reflections and 6-80 for high-angle reflections), either by keeping the incident beam and detector direction fixed and rotating the specimen and detector (the detector at twice the angular velocity) or by keeping the specimen fixed and rotating the incident beam and detector in opposite senses. In both cases this instrumental set-up preserves the symmetrical arrangement [45].

2.6 Antibacterial activity of silver nanoparticles

It is well known that silver ions and silver nanoparticles are highly toxic to microorganisms showing strong biocidal effects on bacteria including *Staphylococcus aureus (S. aureus)* and *Escherichia coli (E. coli).* [2-5, 8, 9, 24, 49-57]

Compared with silver compounds, the mechanism for the antimicrobial activity of silver nanoparticles may be the same, although neither is properly understood. However, because of the large surface area to volume ratio, silver nanoparticles may have much better efficiency. The possible mechanisms of the antibacterial activity are as follows [49-51]:

1. Better contact with the microorganism, silver nanoparticles provides and extremely large surface area for contact with bacteria. The silver nanoparticles get attached to the cell membrane and also penetrate inside the bacteria.

2. Bacterial membranes contain sulfur-containing proteins. Silver nanoparticles, like silver ion (Ag^+), can interact with them as well as with phosphorus-containing compounds like DNA, perhaps to inhibit function.

3. Silver nanoparticles or Ag^+ can attack the respiratory chain in bacterial mitochondria and lead to cell death.

4. Silver nanoparticles can have sustained release of silver ion once inside the bacterial cells (in an environment with lower pH), which may create free radicals and induce oxidative stress, thus further enhancing their bactericidal activity (Figure 2.5) [51].
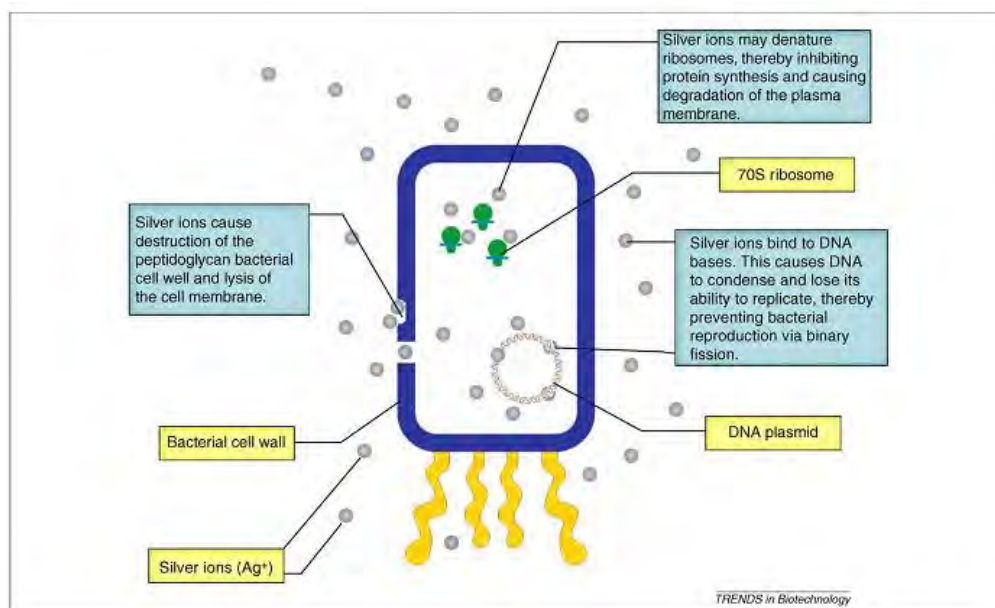
Figure 2.5 The various mechanisms of the antibacterial activity of silver nanoparticles [51].

Summary of the factors affecting AgNPs toxicity are shown in Table 2.4 [53]. Many publications have shown size-dependent toxicities of AgNPs [58-60]. As particle size decreases, the specific surface area increase leaving a higher number of atoms exposed on the surface available for redox, photochemical, and biochemical reactions. One of the key mechanisms for AgNPs to exert antibacterial activity is through the release of silver ions. As the rate of ion release is proportional to particle surface area, nanoparticles can release ions more rapidly than larger particles and macroscopic materials. Silver nanoparticle shape may also be a factor [53, 57]. High atom densities at <111> facets increased the toxicity of AgNPs to bacterial strains. Truncated triangular nanoplates exert stronger antibacterial activity than spherical AgNPs and rod-shaped AgNPs because they contain more <111> facets. The antibacterial properties of AgNPs are related to both size (surface area) and crystallinity (surface reactivity). Stability of AgNPs also influences toxicity since the formation of aggregates tends to decrease biocidal activity. However, water chemistry also governs silver dissolution and/or re-precipitation through various possible redox and precipitation reactions.

Table 2.4 Summary of the factors affecting silver nanoparticles toxicity [53].

Factor	Tendency	Possible explanation
Particle size	Smaller particles sizes tend to enhance antibacterial properties.	As size decrease, there is larger number of atoms on the surface available to interact with bacteria or to release a higher amount of silver ions.
Particle shape	Particles with shapes containing more <111> facets like triangular particles tend to have strongest antibacterial properties.	<111> facets would contain larger atom densities thus more atoms available for interaction.
Particle stability	Higher stability produces a higher antibacterial property.	Non-stable nanoparticles will tend to form aggregates thus surface area will be reduced and the density of atoms available on the surface will be lower.
Water chemistry	Depending in a case to case base.	Since water chemistry affects particle suspension/solubility, particle size distribution, as well as, bacterial ability to face environmental stresses, water chemistry will affect the interaction between silver nanoparticles and bacterial thus influencing the resulting toxicity.

CHAPTER III

EXPERIMENT

3.1 Chemicals and materials

Silver nitrate ($AgNO_3$), sodium hydroxide (NaOH), nitric acid (HNO_3, 65% w/v or v/v), sodium borohydride ($NaBH_4$) and soluble starch were purchased from Merck (Thailand). All Chemicals were analytical grade and were used as received without an additional purification. Tapioca was the product of Thai Wah Products Public Co., Ltd. (Sathorn, Bangkok, Thailand). De-ionized water was used as solvents. All glassware and magnetic bars were thoroughly cleaned with detergent, rinsed with de-ionized water, rinsed with dilute nitric acid (6 M), and thoroughly rinsed again with de-ionized water. Silver salt stock solution (1,000 ppm Ag^+ or 0.01 M Silver ion) was prepared by dissolving silver nitrate ($AgNO_3$) 0.16 g in 100 mL de-ionized water. The solution was stirred until silver nitrate was completely dissolved.

3.2 Green synthesis of silver nanoparticles using tapioca

Silver nanoparticles were synthesized by chemical reduction using tapioca as both reducing agent and stabilizer (as shown in Figure 3.1). Aqueous solution of tapioca was prepared by dissolving 0.1 g of tapioca in 100 mL of de-ionized water and brought to boiling for some minutes. Then, tapioca solution was hydrolyzed by adding 5 mL of 0.1 M HNO_3 and incubated for 20 minutes. Alkaline degradation was carried out by adding 0.1 M NaOH with different volume of NaOH at 5, 10, 15, 20, 25, 30, 40, and 50 mL, respectively and incubated solution for 40 minutes. 10 mL of 1,000 ppm silver salt solution was added to tapioca solution after treating by acid hydrolysis and alkaline degradation. The solution was vigorously stirred and heated at 80 °C for 10 minutes. The color of solution turned brown after reaction was completed, indicating the formation of silver nanoparticles. The total volume was kept

constant at 100 mL by addition of de-ionized water. Finally, the 100 ppm (1 mM) of AgNPs solutions were stabilized with 0.1% w/v tapioca which give colloid S1, S2, S3, S4, S5, S6, S7 and S8, respectively. The time-dependent study on the generation of the generated reducing species by alkaline-degradation of tapioca was conducted from 0.5 to 15 min incubation time.
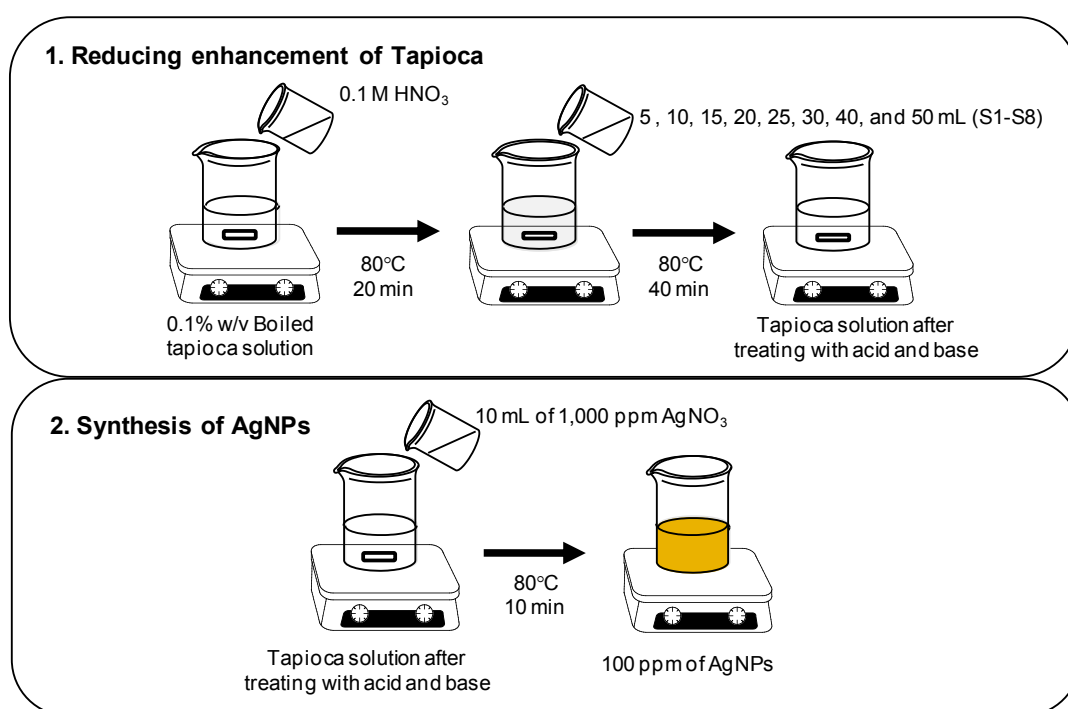
Figure 3.1 Synthesis of silver nanoparticles using tapioca.

3.3 Investigation of various factors affecting the green synthesis of silver nanoparticles

In this method, size, size distribution, and morphology of silver nanoparticles depend on the various reaction conditions such as concentration of tapioca, concentration of silver nitrate, and the reaction temperature.

3.3.1 The concentration of tapioca

The concentrations of tapioca were varied as follows: 0.05, 0.1, 0.2, and 0.5% w/v. The concentration of silver nitrate was maintained at 100 ppm. 10 mL of 1,000

ppm silver nitrate solution was added to tapioca solution after treating by acid hydrolysis and alkaline degradation. Stirred solution vigorously and heated at 80 °C for 10 minutes. The total volume was kept constant at 100 mL by adding of de-ionized water.

3.3.2 The concentration of silver nitrate

The concentrations of silver nitrate were varied as follows: 25, 50, 100, 200, and 500 ppm. The concentration of tapioca was maintained at 0.1% w/v. Aqueous solution of tapioca was prepared by dissolving 0.1 g of tapioca in 100 mL of de-ionized water and brought to boiling for some minutes. Then hydrolyzed tapioca solution by adding 5 mL of 0.1 M HNO_3 and incubated solution for 20 minutes. Making alkaline degradation by adding 20 mL of 0.1 M NaOH and incubated solution for 40 minutes. 2.5, 5, 10, 20, and 50 mL of 1,000 ppm silver salt solution was added to tapioca solution after treating by acid hydrolysis and alkaline degradation. Stirred solution vigorously and heated at 80 °C for 10 minutes.

3.3.3 The reaction temperature

To study the effect of temperature on the synthesized silver nanoparticles, reaction temperature was varied as follows: room temperature, 40, 50, 60, 70, 80, 90, and 100 °C. The concentration of silver nitrate and tapioca were maintained at 100 ppm, and 0.1% w/v, respectively. Aqueous solution of tapioca was prepared by dissolving 0.1 g of tapioca in 100 mL of de-ionized water and brought to boiling for some minutes. Then hydrolyzed tapioca solution by adding 5 mL of 0.1 M HNO_3 and incubated solution for 20 minutes. Making alkaline degradation by adding 20 mL of 0.1 M NaOH and incubated solution for 40 minutes. 10 mL of 1,000 ppm silver salt solution was added to tapioca solution after treating by acid hydrolysis and alkaline degradation. Stirred solution vigorously and heated at various temperatures such as room temperature, 40, 50, 60, 70, 80, 90, and 100 °C for 10 minutes.

3.4 Characterization of synthesized silver nanoparticles

The synthesized silver nanoparticles were characterized by various techniques. Strong surface plasmon resonance peaks were observed by UV-vis spectroscopy. The average size and size distribution of the synthesized silver nanoparticles were investigated by transmission electron microscopy (TEM). The crystal structure of the synthesized silver nanoparticles were elucidated by X-ray diffraction (XRD). The degradation of tapioca *via* an acidic and alkaline treatment were investigated by attenuated total reflection Fourier transform infrared spectroscopy (ATR FT-IR).

3.4.1 UV-vis spectroscopy

Solution of AgNPs was diluted to 10 ppm with de-ionized water before analyzing. A reference of pure de-ionized water was collected as the blank sample. The absorption spectra of the colloidal AgNPs were carried out on Ocean Optics Portable UV-visible spectrometer. The light source of this instrument was deuterium lamp (DH-2000, Micropack, bandwidth 200-850 nm). The USB 2000 spectrophotometer was used as detector. The quartz cuvette with optical path length of 1.0 cm was employed as a sample cell and washed by de-ionized water before collecting the spectrum.

3.4.2 ATR FT-IR spectroscopy

A Nicolet 6700 FT-IR spectrometer attached to the Continuum infrared microscope, which equipped with a mercury-cadmium-telluride (MCT) detector, with a built-in 15X Schwarzschild-Cassegrain infrared objective was employed for the spectral acquisition of molecular information of tapioca and tapioca stabilized-AgNPs. A homemade slide-on Ge μATR accessory with a cone shape Ge IRE was employed as a sampling probe. To collect an infrared spectrum, tapioca solution and tapioca-stabilized AgNPs colloid were dropped onto a glass slide and dried under the ambient condition. The dried film on the glass slide was mounted onto the sample stage beneath the infrared objective. The spectral acquisition at a defined position was conducted by raising the sample stage until the dried film on the glass slide contacted

the tip of the Ge µIRE. All ATR spectrums were collected at 4 cm^{-1} collection with 128 scans.

3.4.3 TEM

TEM images of synthesized silver nanoparticles were recorded with a Hitachi, H-7650 analytical transmission electron microscope. The colloidal AgNPs were diluted to 50 ppm (0.5 mM) and dropped onto a formvar-coated copper grid. The specimen were dried over night in a desiccator. The accelerating voltages of this instrument are 100 kV. The histogram of silver nanoparticles size distribution and average diameter of nanoparticles were determined by counting of 300 particles from the TEM image using Image J software while data were analyzed by means of the software OriginPro 8.

3.4.4 XRD analysis

The synthesized silver nanoparticles were dried at 80 °C, and the brown-coloured powder obtained was used for XRD analysis. The powder XRD pattern was obtained with a Rigaku RINT2000 X-ray diffractometer using Cu Kα_1 radiation (λ = 0.154 nm) and a power of 40 kV and 20 mA. The diffracted intensities were recorded from 30° to 80° 2θ angles.

3.5 Long term stability of synthesized silver nanoparticles

The synthesized silver nanoparticles were kept at room temperature. UV-vis analysis of several weeks of old samples was also carried out to check the stability of silver nanoparticles.

3.6 Comparison of synthesized silver nanoparticles reduced with tapioca and soluble starch

UV-vis extinction spectra of synthesized silver nanoparticles using tapioca, and soluble starch were measured. The results were compared to investigate the size and size distribution of silver nanoparticles.

3.7 Comparison of green synthesis method and sodium borohydride method

UV-vis extinction spectra of synthesized silver nanoparticles via green synthesis method (100 ppm AgNPs with 0.1% tapioca) and sodium borohydride method (5,000 ppm of AgNPs with $NaBH_4$ and 2% w/v soluble starch and 5,000 ppm of AgNPs with $NaBH_4$ and 6% w/v polyvinylpyrrolidone) were measured. The results were compared to investigate the size and size distribution of silver nanoparticles.

5,000 ppm of AgNPs with $NaBH_4$ and 2% w/v soluble starch was synthesized. Briefly, a 0.094 M aqueous solution of $AgNO_3$ was prepared with 2% soluble starch as a stabilizer. An aqeous solution of 0.07 M $NaBH_4$ with the soluble starch solution as a solvent was prepared. By mixing both solutions, $AgNO_3$ solution was added to $NaBH_4$ solution under vigorous stirring. When all reactants were completely added, the solution turned dark brown.

5,000 ppm of AgNPs with $NaBH_4$ and 6% w/v PVP was synthesized by the same method that mentioned above but used ethyl alcohol as solvent.

3.8 Antibacterial activity of synthesized silver nanoparticles

The antibacterial activity of synthesized silver nanoparticles against *Escherichia coli* ATCC 25922 and *Staphylococcus aureus* ATCC 25923 were investigated as a model for Gram-negative and Gram-positive bacteria. Bacteriological tests were performed on solid nutrient agar (Difco^{TM}) plates and in liquid systems supplemented with different concentrations of silver nanoparticles.

To examine the bactericidal effect of silver nanoparticles approximately 10^6 colony-forming units (CFU) of *Escherichia coli* ATCC 25922 were cultured on

nutrient agar (Difco^{TM}) plates supplemented with silver nanoparticles in concentrations of 2.5, 5, and 10 ppm (μg/mL). Silver-free agar plates cultured under the same conditions were used as a control. The plates were incubated for 24 h at 37 °C and the numbers of colonies were counted. The counts on the two plates corresponding to a particular sample were averaged. The percentage reduction in bacterial count was calculated by the equation:

$$\% \text{ reduction} = \frac{(\text{viable CFU at 0 hour} - \text{viable CFU at 24 hour})}{\text{viable CFU at 0 hour}} \times 100$$

CHAPTER IV

RESULTS AND DISCUSSION

4.1 Green synthesis of silver nanoparticles using tapioca

The formation of the synthesized silver nanoparticles was investigated using UV-visible spectroscopy, which demonstrated for the analysis of nanoparticles formation over time. The color of the obtained solutions at different volumes of NaOH including UV-visible spectrum of each condition is shown in Figure 4.1A. Though tapioca has been evaluated to use both as reducing agent and stabilizer in the preparation of silver nanoparticles, no silver nanoparticles appeared at 5 mL of NaOH (S1). The solution was colorless and there was no surface plasmon band in the spectrum. We found that increased the amount of NaOH did influence the formation of silver nanoparticles as the typical peak at ~400 nm corresponding to the characteristics of surface plasmon resonance of silver nanoparticles were observed and the color of solution was rapidly changed from colorless to dark brown (S1-S8). This confirms that the silver nanoparticles are formed. The observed plasmon band was very symmetric, which indicates that there are not any aggregated particles in the solution. Stability of silver nanoparticles was investigated by staying the solutions at room temperature for one week (as shown in Figure 4.1B). The plasmon band of solution (S7-S8) was shifted to higher wavelength (Red shift) about 570 nm which suggests that there are some aggregated particles. This may be due to excess bases which decomposed the tapioca operated as the protecting agent.
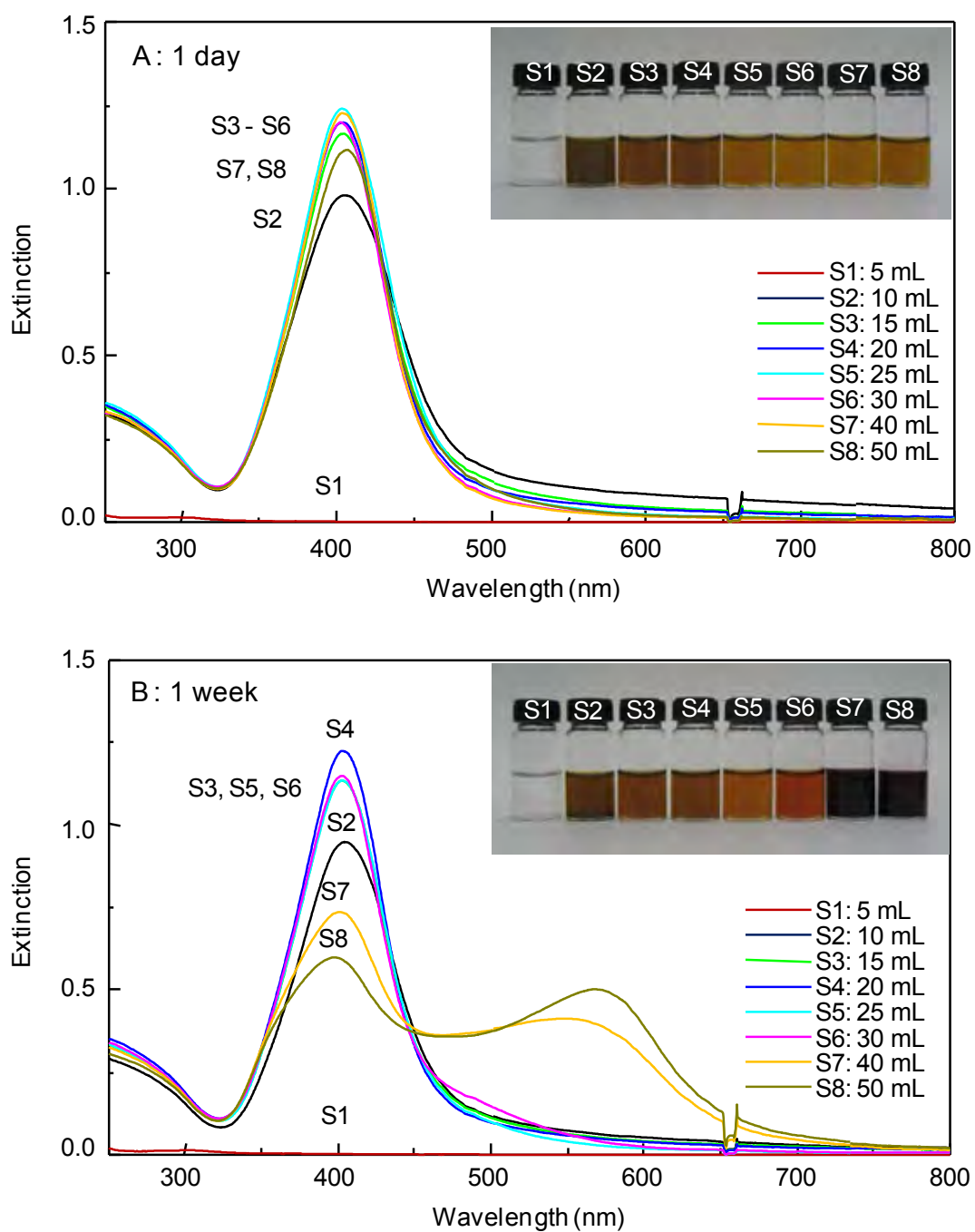
Figure 4.1 The plasmon extinction spectra of silver nanoparticles (S1-S8) prepared at different volumes of NaOH (5, 10, 15, 20, 25, 30, 40, and 50 mL, respectively). Inset photo shows the color of silver nanoparticles changes with volume of NaOH. (A: 1 day, B: 1 week)

Plot of the intensity of the surface plasmon at extinction maximum against the volume of NaOH was shown in Figure 4.2.
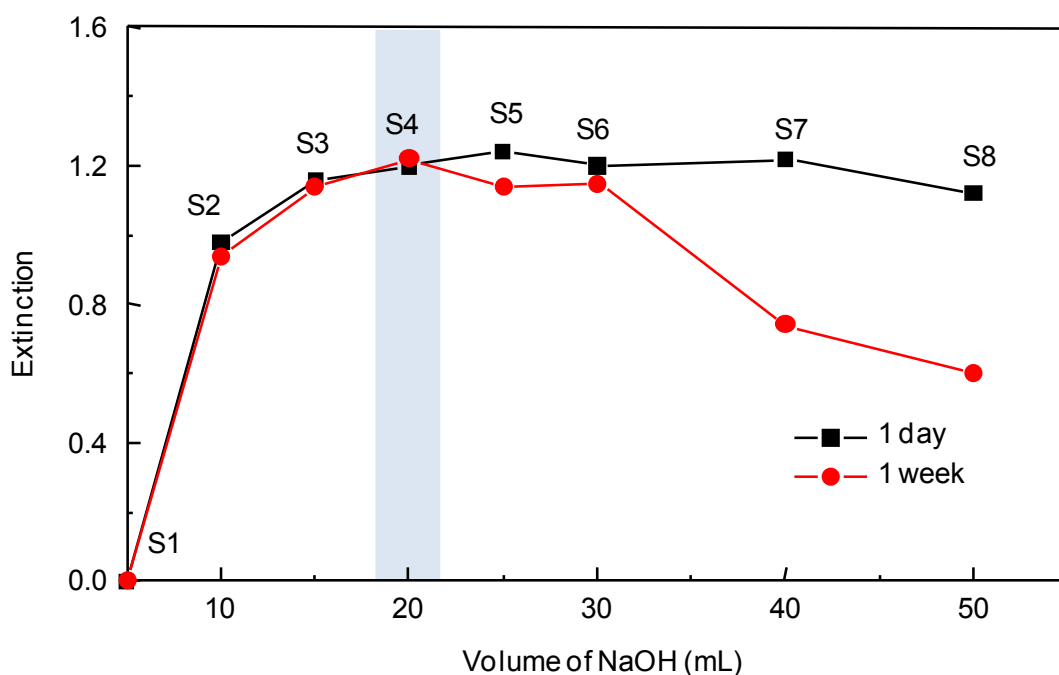
Figure 4.2 Plot of the intensity of the surface plasmon at extinction maximum against the volume of NaOH.

The adequate volume of 0.1 M NaOH at 20 mL was considered as the appropriate condition for synthesizing silver nanoparticles with high stability. The maximum of extinction spectrum (λ_{max}) of AgNPs (S4) was at 400 nm with a narrow full width at half maximum (FWHM) about 70 nm. This result indicated that the size distribution of AgNPs was narrow (as shown in Figure 4.3 A). The plasmon band of AgNPs (S8) was shifted to higher wavelength (Red shift) about 570 nm which suggests that there are some aggregated particles (as shown in Figure 4.3 B).

Synthesized silver nanoparticles (S4 and S8) after 1 week were characterized by TEM in order to confirm that S4 which particles are spherical and narrow size distribution and silver nanoparticles (S8) were aggregated.
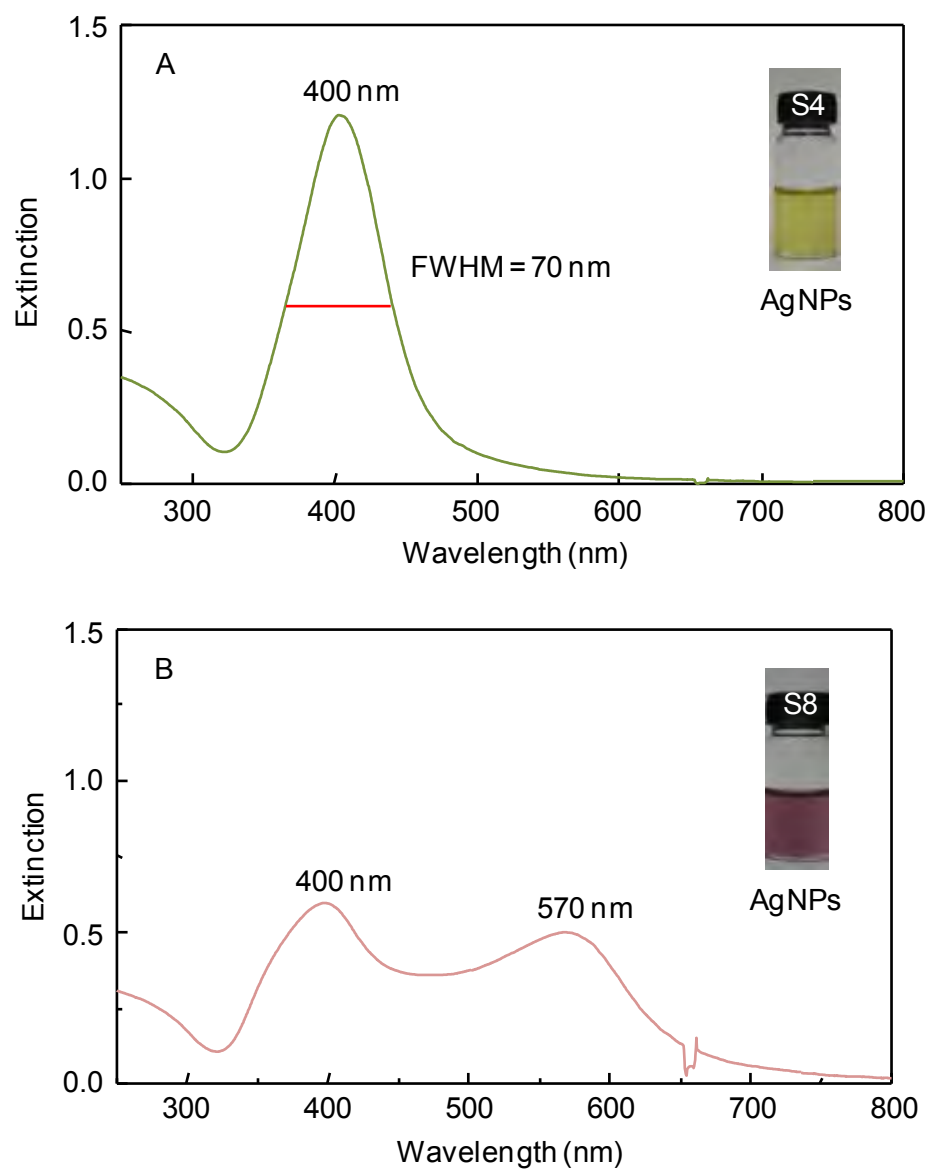
Figure 4.3 The plasmon extinction spectrum of synthesized silver nanoparticles (A: S4 and B: S8) after 1 week.

TEM images of synthesized silver nanoparticles (S4) are shown in Figure 4.4. TEM measurements were used to determine the morphology and shape of nanoparticles.
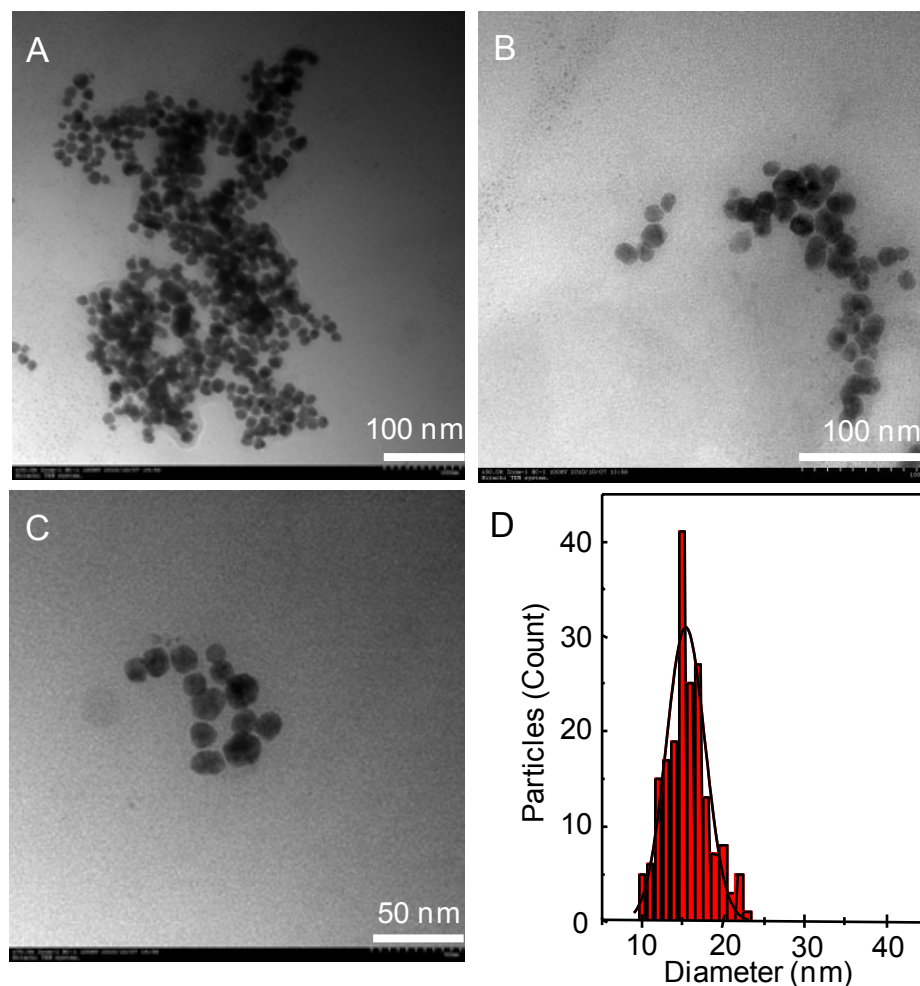
Figure 4.4 (A)-(C) TEM images of synthesized silver nanoparticles (S4); (D) Size distribution histogram.

The particles are spherical in shape with uniform size distribution. The particle size ranged from 10 to 23 nm and the histogram showed the particle size distribution of the synthesized silver nanoparticles (the average particles size = 15.3 nm, σ = 2.4 nm).

TEM images of synthesized silver nanoparticles (S8) are shown in Figure 4.5.
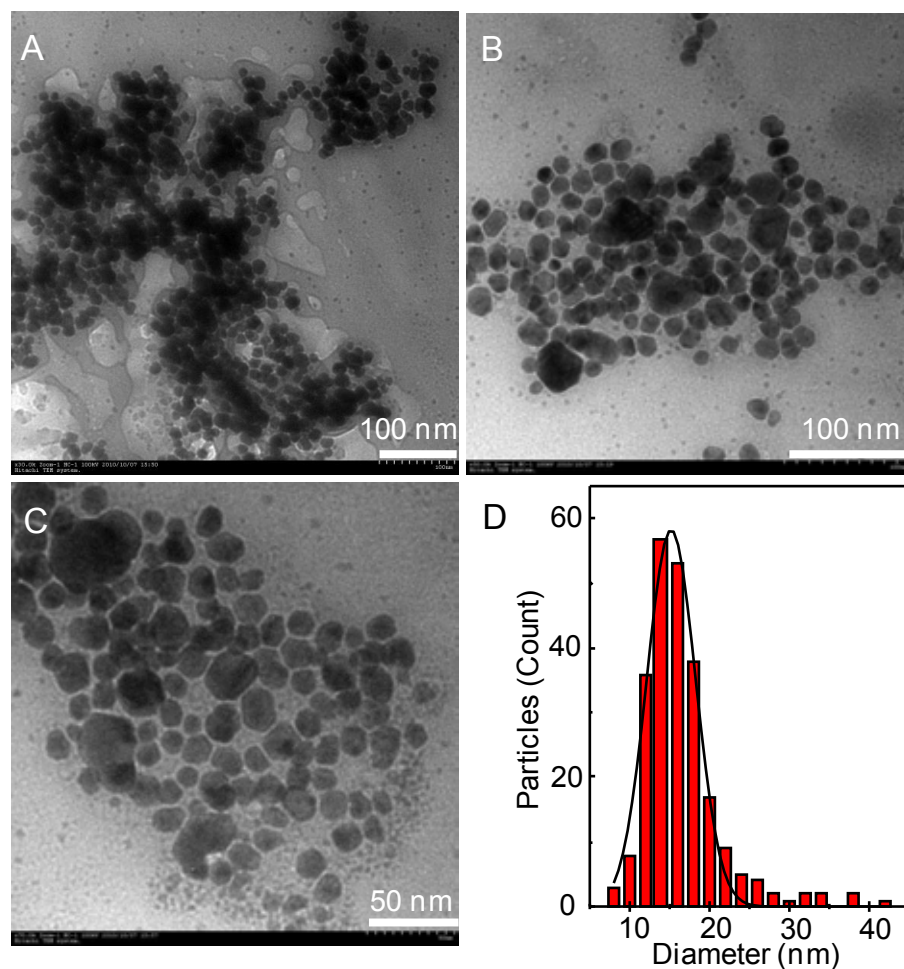
Figure 4.5 (A)-(C) TEM images of synthesized silver nanoparticles (S8); (D) Size distribution histogram.

All of the particles are nearly spherical in shape. The nanoparticles appear to aggregate and form nanoplate. It indicated that shape had been changed but plasmon band did not occur at 340 nm (plate characteristic of transverse quardrupole). The particle size ranged from 10 to 52 nm and histogram showed the particle size distribution of the synthesized silver nanoparticles (the average particles size = 15.8 nm, σ = 2.2 nm).

4.2 The silver nanoparticles growth kinetics

The time-dependent study on the generation of the generated reducing species by alkaline-degradation of tapioca was conducted with 0.5 to 15.0 min incubation time.

To evaluate the correlation between reduction time and particle growth, the reduction reaction was determined by sampling solution at defined time and analyzed with UV-vis spectroscopic technique. The time-resolved plasmon extinction spectra of the synthesized silver nanoparticles solution are shown in Figure 4.6.
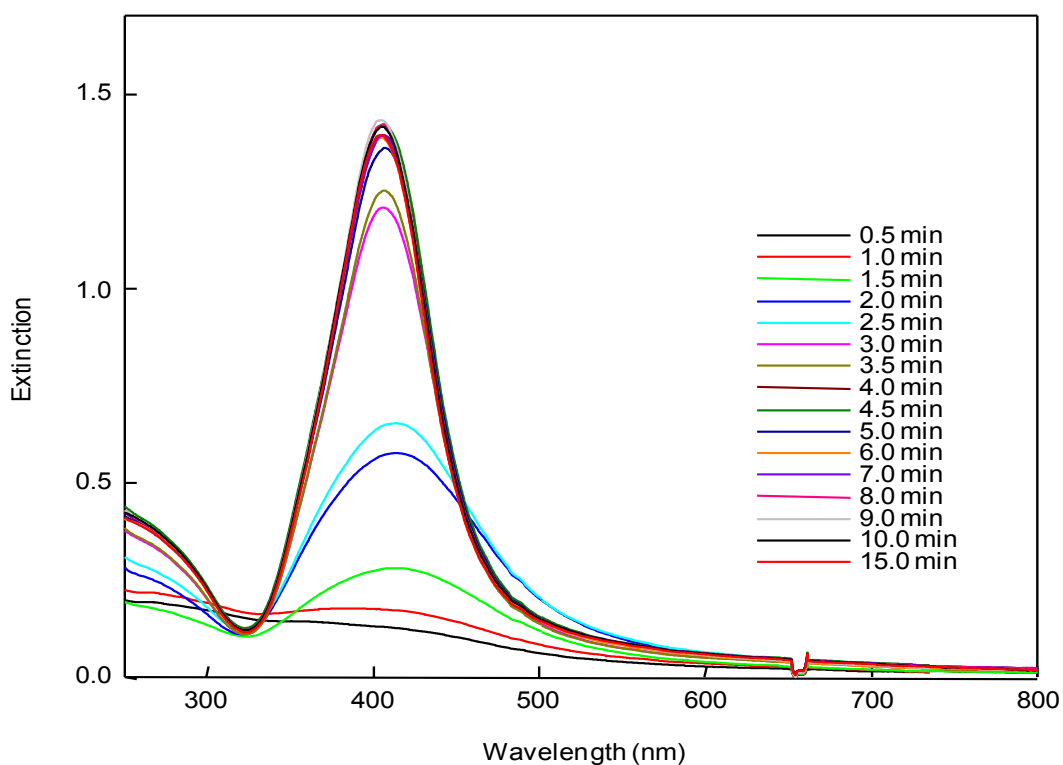
Figure 4.6 Time-resolved plasmon extinction spectra of synthesized silver nanoparticles (S4).

The plasmon extinction at ~400 nm from all spectra in Figure 4.6 were plotted against time as shown in Figure 4.7.
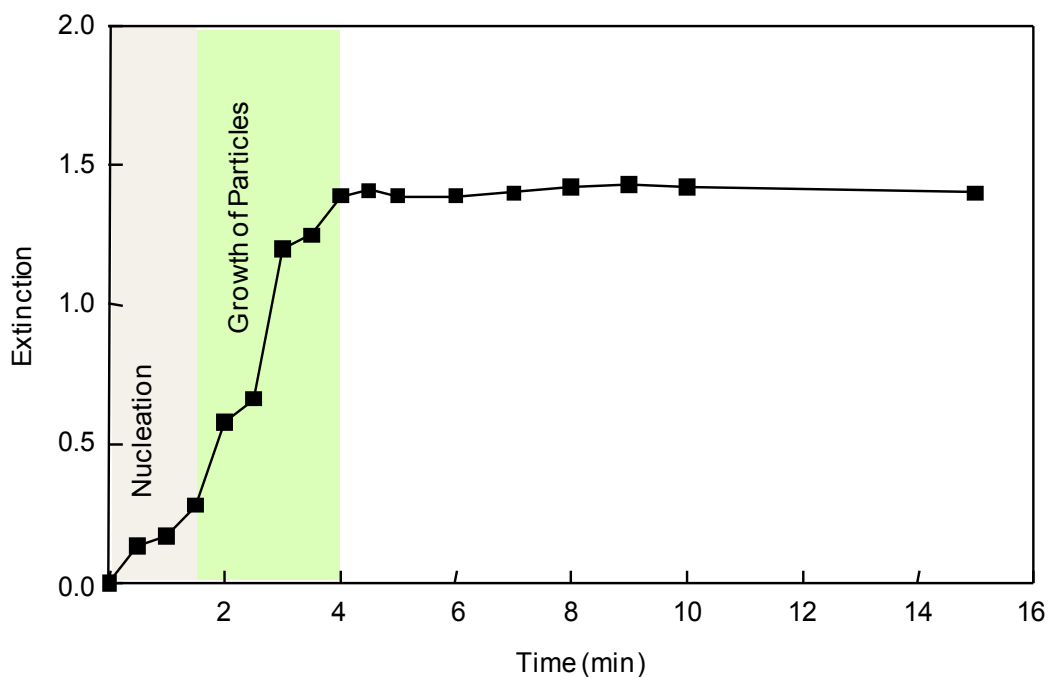
Figure 4.7 Time-dependent plasmon extinction at plasmon maxima of the synthesized silver nanoparticles (S4).

In order to investigate the reducing efficiency of the generated species, a time dependent UV-vis experiment was conducted and the results are shown in Figure 4.7. When the time increased to 1.5 min, the extinction slightly increased and dramatically increased as the reduction time reached to 4 min and nearly constant till 10 min before showing no significant change. The reduction profile show sigmoidal shape. An increasing absorbance in the first period corresponded to the seed nucleation, followed by a rapid particle growth (as suggested by LaMer [61] in colloidal growth mechanism). In our case, due to the high efficiency of the generated reducing species, the nucleation is very fast and the reaction was completed within 10 min.

As the above results, it suggested that tapioca treated with 20 mL of 0.1 M NaOH having enough reducing power to convert silver ion to silver particles and the reduction reaction were almost complete at 10 min.

4.3 Investigation of various factors affecting the green synthesis of silver nanoparticles

In this method, size, size distribution, and morphology of silver nanoparticles depend on the various reaction conditions such as concentrations of tapioca, concentrations of silver nitrate, and the reaction temperatures.

4.3.1 The concentrations of tapioca

The concentrations of tapioca were varied as follows: 0.05, 0.1, and 0.2% w/v.
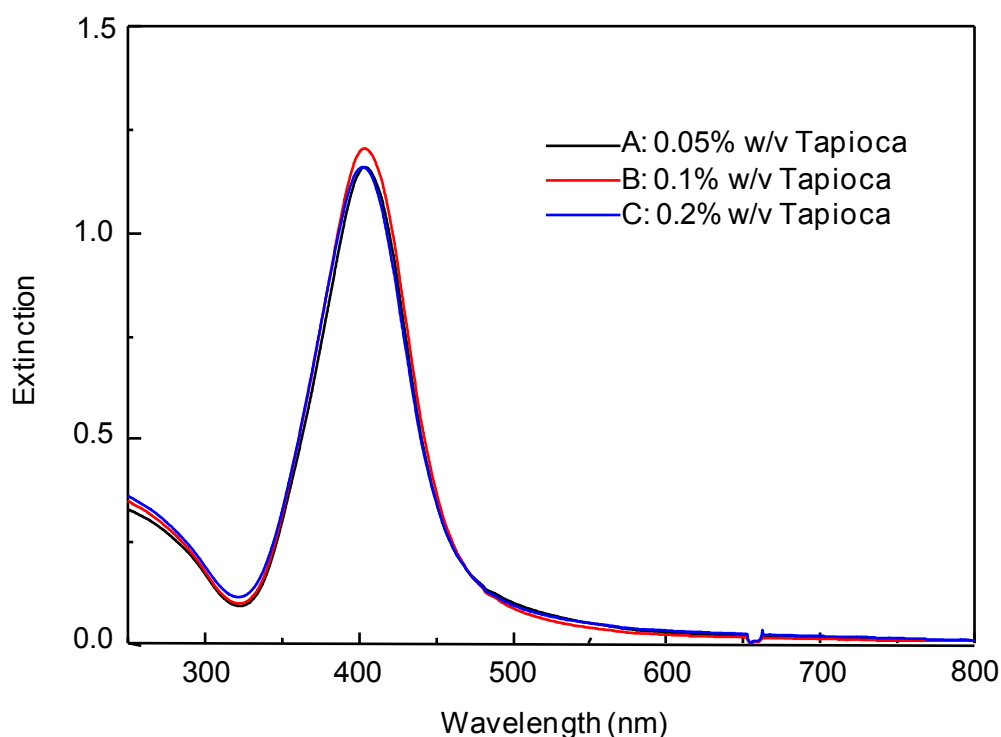
Figure 4.8 The plasmon extinction spectra of synthesized silver nanoparticles reduced with various concentrations of tapioca. (A: 0.05, B: 0.1, and C: 0.2% w/v)

When the concentration of tapioca was increased, and insignificant change was observed in the position and shape of plasmon extinction. The plasmon extinction maxima of all samples appeared at about 400 nm, as shown in Figure 4.8. After 2 weeks, the silver nanoparticles with 0.05% w/v tapioca were precipitated. We

concluded that the aggregation was due to an inadequate stabilization power of low concentration tapioca. It is possible that there are enough reducing species but the tapioca concentration is too low to stabilized silver nanoparticles. Silver nanoparticles with 0.1 and 0.2% w/v tapioca, the colloid did not precipitate. This implied that there was enough starch molecules to stabilize silver nanoparticles.

4.3.2 The concentrations of silver nitrate

The concentrations of silver nitrate were varied as follows: 25, 50, 100, 200, and 500 ppm. The concentration of tapioca was maintained at 0.1% w/v. Figure 4.9 shows the normalized extinction spectra of the synthesized silver nanoparticles with various concentrations of silver nitrate.
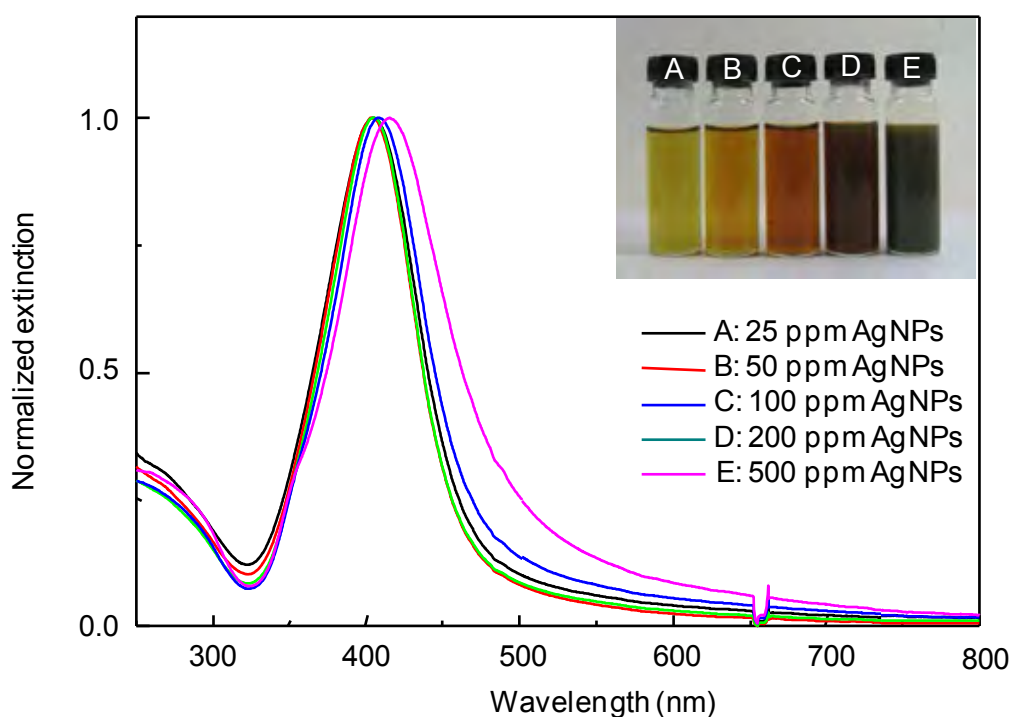
Figure 4.9 The normalized extinction spectra of the synthesized silver nanoparticles with various concentrations of silver nitrate. (A: 25, B: 50, C: 100, D: 200 and E: 500 ppm)

The normalized extinction spectra of the synthesized silver nanoparticles with 25-200 ppm of silver nitrate (A-D), there were no significant change in the position of

the extinction maxima and FWHM. These results imply that the concentrations of silver nitrate affected the amount of silver nanoparticles but did not affect their size, size distribution and morphology. When the concentration of silver nitrate was increased to 500 ppm, the normalized extinction spectrum of synthesized silver nanoparticles showed the extinction maxima at longer wavelength (red shift) and broad spectrum. This indicates that there is the formation of the larger silver nanoparticles. Therefore, silver nitrate concentration was limited at 100 ppm.

4.3.3 The reaction temperature

To study the effect of temperature on the synthesized silver nanoparticles; reaction temperature was varied as follows: room temperature, 40 °C, 50 °C, 60 °C, 70 °C, 80 °C, 90 °C, and 100 °C. The concentration of silver nitrate and tapioca were maintained at 100 ppm, and 0.1% w/v, respectively.
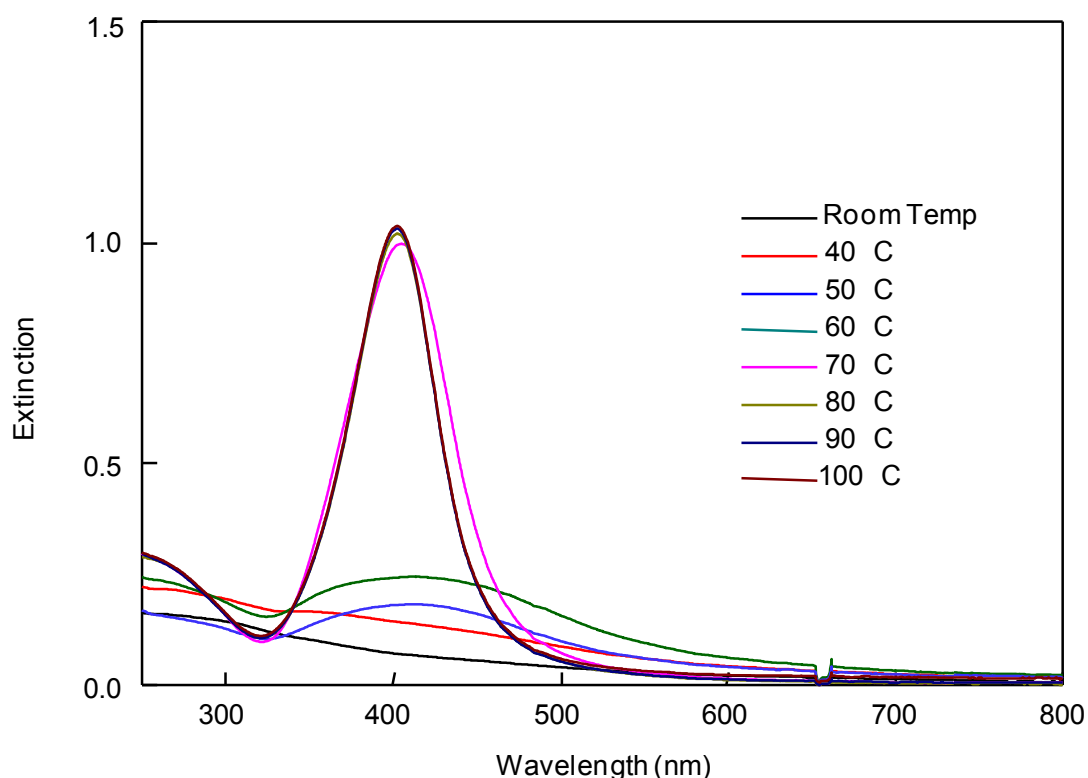
Figure 4.10 The plasmon extinction spectra of the synthesized silver nanoparticles with various reaction temperatures.

Temperature is one of the factors affecting chemical reaction of silver ion. Normally, when reaction is increased, reaction rate is also increased. For silver nanoparticles synthesized by chemical reduction, fast reduction rate trends to produce smaller silver nanoparticles due to the promotion of the nucleation of seeds instead of the growth of particles. This phenomenon also occurred in our green synthesis system as the temperature was increased from room temperature to 100 °C. It is observed that the maximum extinction occurs at about 400 nm. The extinction spectra of silver nanoparticles synthesized with reaction temperature (80, 90 and 100 °C) showed the higher conversion.

4.4 XRD Analysis

XRD pattern of the synthesized silver nanoparticles with optimum condition (0.1% tapioca modified with 5 mL of 0.1M HNO_3 and 20 mL of 0.1M NaOH, reaction temperature 80 °C) was shown in Figure 4.11.
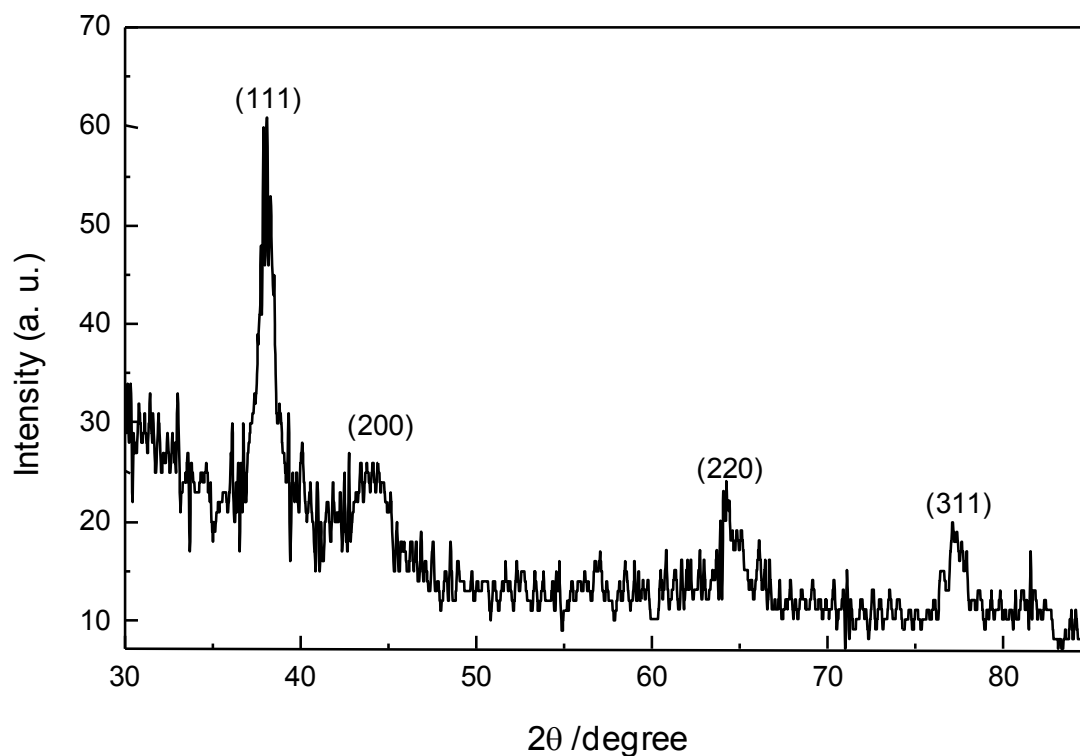
Figure 4.11 X-ray diffraction pattern of the synthesized AgNPs.

The synthesized silver nanoparticles were highly crystalline with diffraction peaks corresponding to the face-centered cubic (fcc) phase of metallic silver. A number of Bragg reflections with 2θ values of 38°, 45°, 64°, and 77° sets of lattice planes are observed which may be indexed to the (111), (200), (220), and (311) facets of the fcc structure of metallic silver. No extra diffraction peaks (impurities or oxides) were present, suggesting that the synthesized silver was essentially pure.

4.5 The effect of acidic-alkaline treatment on the degradation of tapioca

In order to investigate the effect of acidic-alkaline treatment on the degradation of tapioca; the solution was analyzed by attenuated total reflection Fourier transform infrared spectroscopy (ATR FT-IR). In Figure 4.12, ATR FT-IR spectra of tapioca solution, tapioca after treated with acidic and alkaline and tapioca in silver colloid were compared.
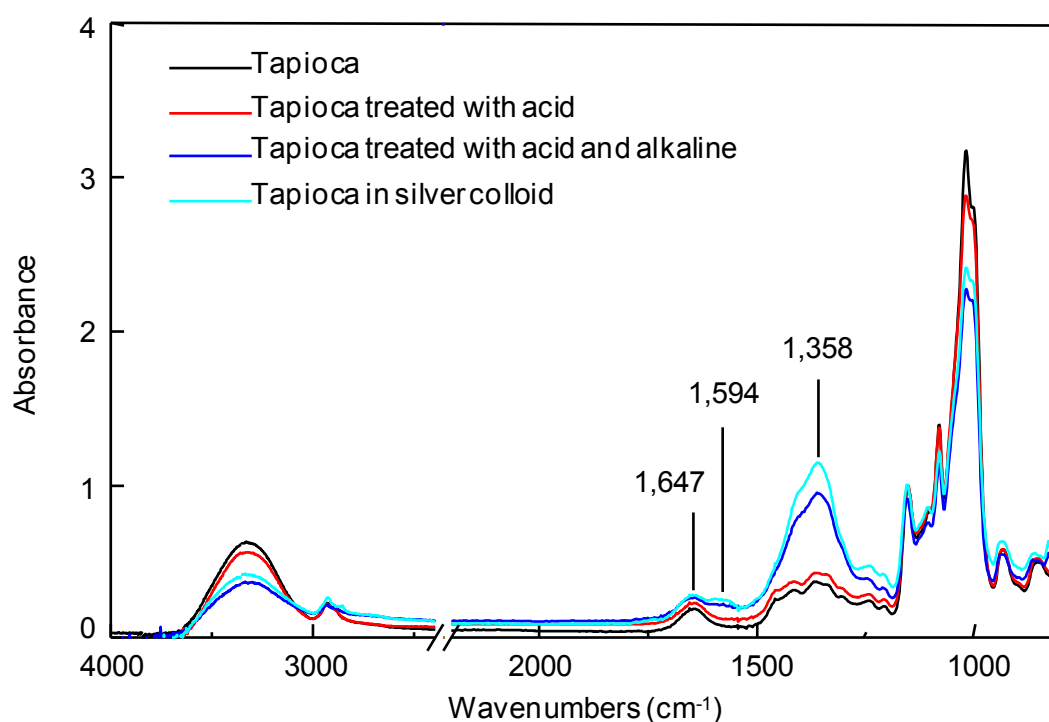
Figure 4.12 Normalized ATR FT-IR spectra of tapioca, tapioca treated with acid, tapioca treated with acid and alkaline, and tapioca in silver colloid.

The broad absorption band from 3,600 to 3,000 cm^{-1} are according to the –OH stretching vibration and band at 2,900 cm^{-1} is attributed to C-H stretching modes. An absorption band at 1,647 cm^{-1} is assigned to water adsorbed in the amorphous starch [62]. Under the acidic treatment, the ATR FT-IR spectra of tapioca showed that the long chain hydrocarbon could be only hydrolyzed to short chain but the structure does not change (glycosidic linkage of starch bridge β C^1-O-C^4 in the region 1,200–900 cm^{-1}). The confirmation of the breaking of the glycosidic bonds is the exits of the high number of end aldehyde groups which agreeable to the ATR FT-IR spectrum [63]. When the tapioca was under alkaline treatment, a significant change of ATR FT-IR spectra of tapioca was observed by the development of absorption band at 1,594 cm^{-1} and 1,358 cm^{-1} attributed to –COO$^-$ asymmetrical and symmetrical stretching vibration, respectively [64]. This absorption band is expected to associate with generated reducing species upon degradation of tapioca molecules. The drastically change in the spectral envelop in 1,200 - 900 cm^{-1} which associated with the main structure of tapioca, was significantly changed.

The observed spectral change agreed with that of the alkaline degradation of polysaccharide given by the Nef-Isbell mechanism [65-68]. The detail infrared band assignment is shown in Table 4.1.

Table 4.1 Infrared spectra band assignments of starch [65-68].

Infrared band (cm^{-1})	Infrared band assignment
860	CH$_2$ deformation
930	Skeleton mode vibration of α-1,4 glycosidic linkage (C-O-C)
1200 – 900	Bridge β C^1-O-C^4 stretching
1500 – 1300	Vibration band related to the carbon and hydrogen atoms
1610 – 1550/1420-1300	COO$^-$ stretching vibration (carboxylic acid salt)
1642	Water adsorbed in the amorphous region of starch
1765	C=O stretching vibration of carboxylic acid
3000 – 2800	C-H stretching
3600 - 3100	O-H stretching

In this work, tapioca, a linear polymer of glucose units, was used as both the reducing and the stabilizing agent. The degradation of starch under alkaline treatment involves a β-elimination reaction followed by a series of rearrangement before liberation of a glucose unit. A simplified mechanism of starch degradation is shown in Scheme 4.1 [65-68].

(I)   keto-enol tautomerism
(II)   enediol deprotonation
(III) anion isomerisation
(IV)   β-hydroxycarbonyl elimination
(V)   β-alkoxycarbonyl elimination
(VI)   benzilic acid rearrangement
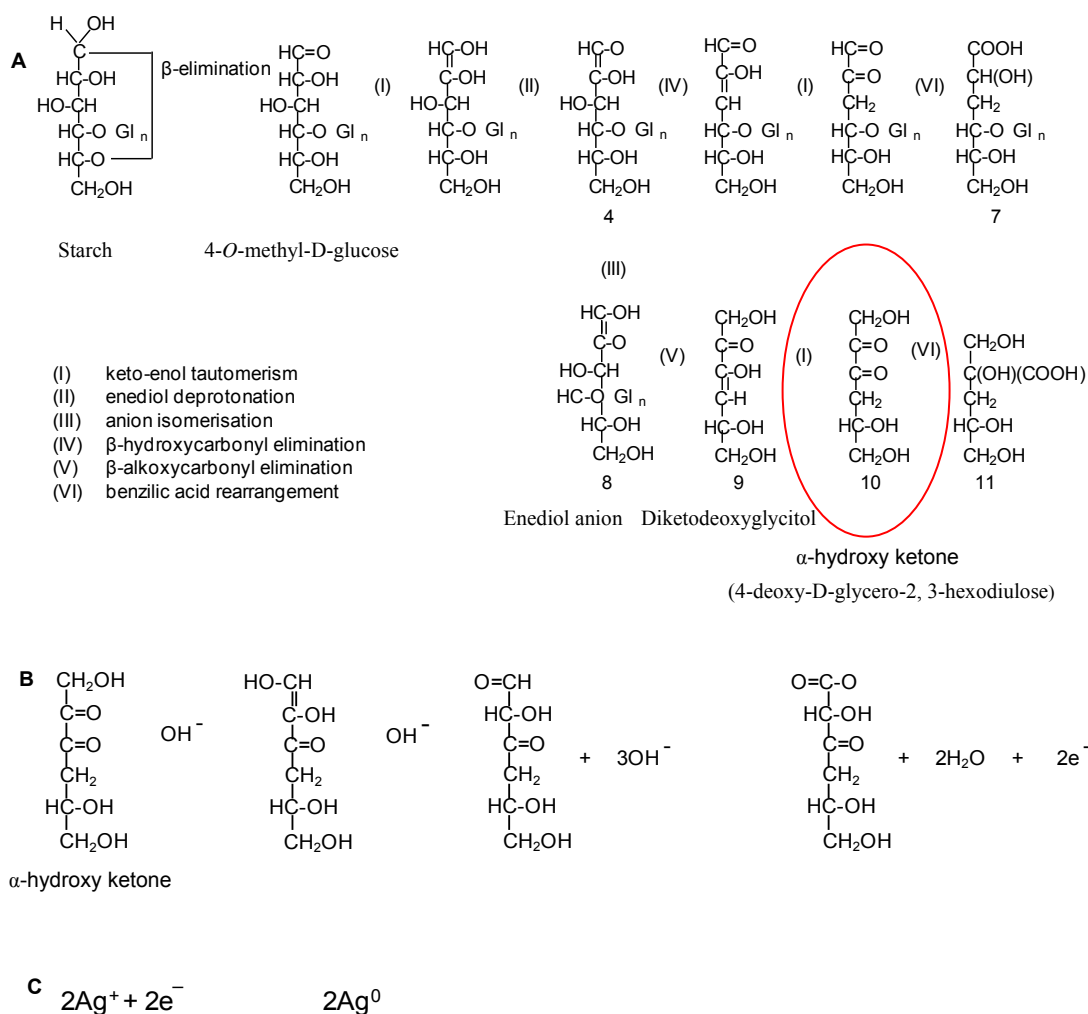
Scheme 4.1 (A) The possible process of starch under alkaline degradation to generate reducing end groups adapted from Nef-Isbell mechanism [65-68]. (B) Example of reducing species (C_6) from degraded intermediates. (C) Reduction of silver ions to silver nanoparticles.

From Scheme 4.1 A, the first step is the ring opening of glucose unit 1 via β-elimination reaction to form 4-*O*-methyl-D-glucose (2). This unit can be formed as enediols (3) via keto-enol tautomerism (i), which is then followed by enediol deprotonation by hydroxide ions (ii) to form the enediol anion (4). After that isomerisation (iii) of anion (4) to (8) followed by reprotonation. Anion (8) has the methoxyl group in the β–position relative to the negative charge of the anion and thus β-alkoxycarbonyl elimination (v) of the enediol anion (8 take places. Therefore, β-alkoxycarbonyl elimination produces a diketodeoxyglycitol product (9). The degradation pathway then continues, keto-enol tautomerism (i) of (9) produces 4-deoxy-D-glycero-2,3-hexodiulose (10 . β-alkoxycarbonyl elimination (v) occurs more readily than β-hydroxycarbonyl elimination (iv). The generations a new deprotonated end groups (e.g., structure (8) and (10)) can undergo further alkaline degradation like monosacharide degradation. M. A. Clarke, et al show that the monosaccharide degradation under an alkaline treatment could generated molecules with carbonyl functionalities [67]. Some of the degraded products show reduction potentials such as those with aldehyde and α-hydroxy ketone functionalities. Aldehyde and α-hydroxy ketone can be efficient reducing specie under the employed alkaline condition (Scheme 4.1 B). As a result, silver ions could be reduced to silver nanoparticles as indicated by Scheme 4.1 C. A simplification of monosaccharide degradation products with different carbon number are shown in Scheme 4.2 [65-68]. Some of the intermediates have aldehyde or α-hydroxy ketone moiety which can function as powerful reducing species under an alkaline condition. There are at least 17 reported reducing species of different carbon number (as shown in Table 4.2).

Scheme 4.2 The reaction pathways of monosaccharide under alkaline degradation. Classification of the degraded products based on carbon number was simplified (adapted from references [63-68]). Some of the degradation intermediates contain functional groups with reduction potential (i.e., aldehyde and α–hydroxy ketone moieties).
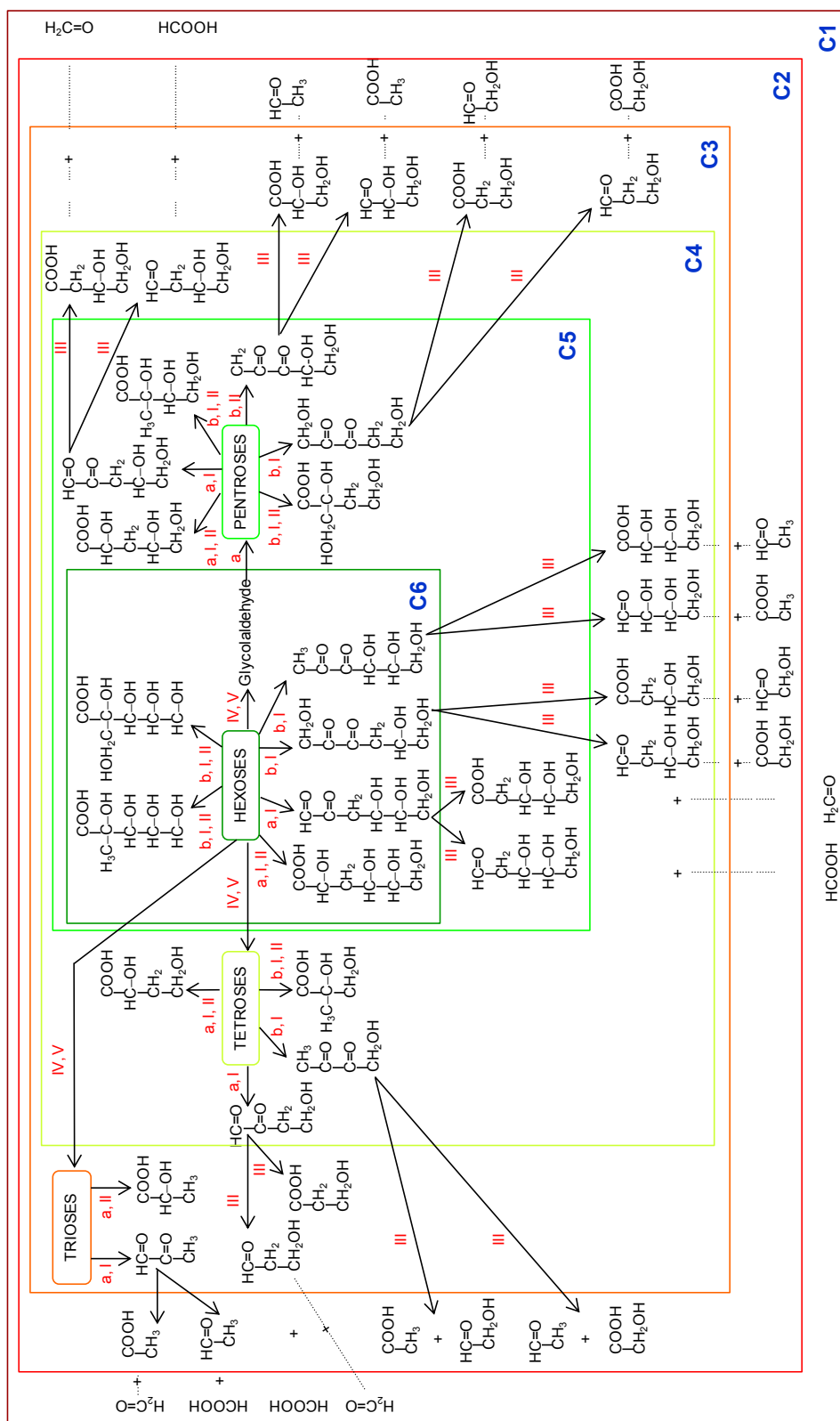
a : 1,2-enediol, b : 2,3-enediol, I : β-elimination, II : benzilic and rearrangement, III : α-dicarbonyl clevage, IV : retro-aldolization, V : aldolization

Table 4.2 The possible degradation products of starch in alkaline solution those act as reducing species [64-68].

Numbers of Carbon	Structure	Product name
6	HC=O C=O CH₂ HC–OH HC–OH CH₂OH	4,5,6-trihydroxy-2-oxohexanal
6	CH₂OH C=O C=O CH₂ HC–OH CH₂OH	1,5,6-trihydroxyhexane-2,3-dione
6	CH₃ C=O C=O HC-OH HC–OH CH₂OH	4,5,6-trihydroxyhexane-2,3-dione
5	HC=O C=O CH₂ HC–OH CH₂OH	4,5-dihydroxy-2-oxopentanal
5	CH₃ C=O C=O HC-OH CH₂OH	4,5-dihydroxypentane-2,3-dione
5	CH₂OH C=O C=O CH₂ CH₂OH	1,5-dihydroxypentane-2,3-dione
5	HC=O CH₂ HC–OH HC–OH CH₂OH	3,4,5-trihydroxypentanal

Table 4.2 The possible degradation products of starch in alkaline solution (continued).

Numbers of Carbon	Structure	Product name
4	HC=O C=O CH₂ CH₂OH	4-hydroxy-2-oxobutanal
4	CH₃ C=O C=O CH₂OH	1-hydroxybutane-2,3-dione
4	HC=O CH₂ HC–OH CH₂OH	3,4-dihydroxybutanal
4	HC=O HC–OH HC–OH CH₂OH	2,3,4-trihydroxybutanal
3	HC=O HC–OH CH₂OH	2,3-dihydroxypropanal
3	HC=O CH₂ CH₂OH	3-hydroxypropanal
3	HC=O C=O CH₃	2-oxopropanal
2	HC=O CH₂OH	2-hydroxyacetaldehyde
2	HC=O CH₃	Acetaldehyde
1	H₂C=O	formaldehyde

4.6 Long term stability of the synthesized silver nanoparticles

The prepared silver nanoparticles (S4) were kept at room temperature and regularly monitored by UV-visible spectroscopy for six months.
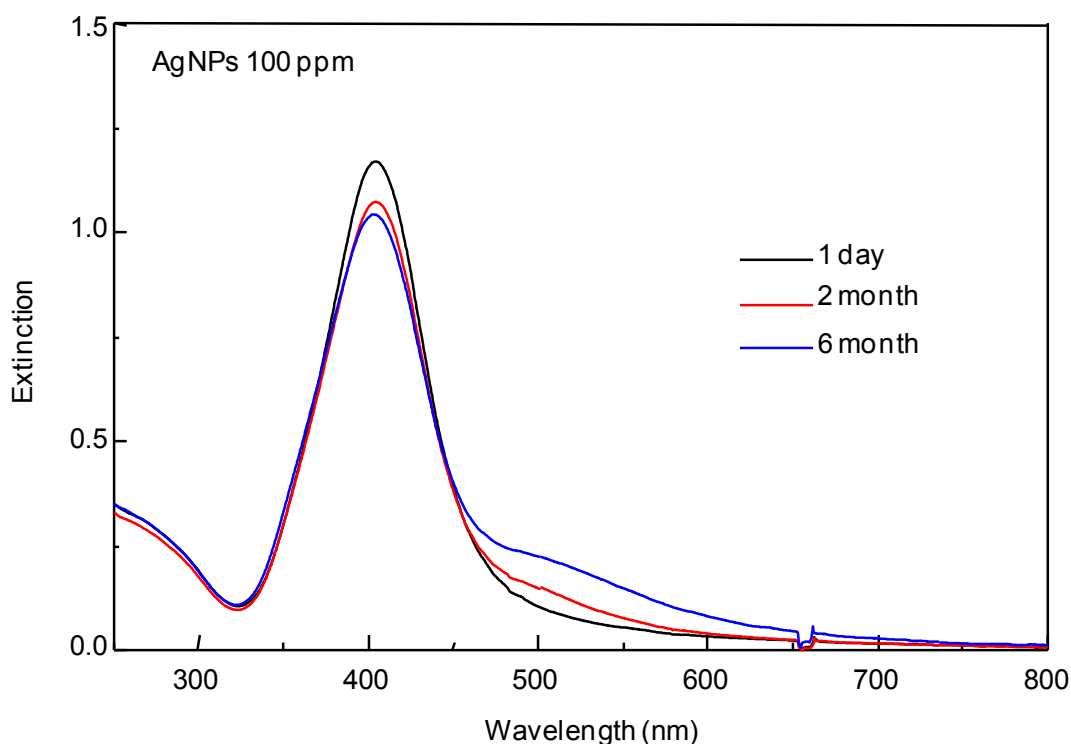
Figure 4.13 Stability of the synthesized silver nanoparticles (S4).

It was noticeable that the colloidal solution of synthesized AgNPs was extremely stable at room temperature, with no evidence of precipitation of particles as determined by UV-visible spectroscopy (Figure 4.13). The intensity of spectrum of synthesized AgNPs measured after two months was decreased. The additional shoulder at about 550 nm was observed. This indicated that the spectrum consists of the broaden size and shape particles in the aggregated system. However, AgNPs were not precipitated in the solution. The tapioca is a linear polymer formed by glucose units, the extensive number of hydroxyl groups present in tapioca can facilitate the complexation of metal ion to molecular matrix that prevent the aggregation of AgNPs

[24]. Moreover, it supposes that the long chain of tapioca structure can stabilize AgNPs via steric hindrance.

4.7 Comparison of the synthesized silver nanoparticles reduced with tapioca and soluble starch

UV-visible extinction spectra of the synthesized silver nanoparticles reduced with tapioca and soluble starch were measured. The results were compared to investigate the size and size distribution of silver nanoparticles.
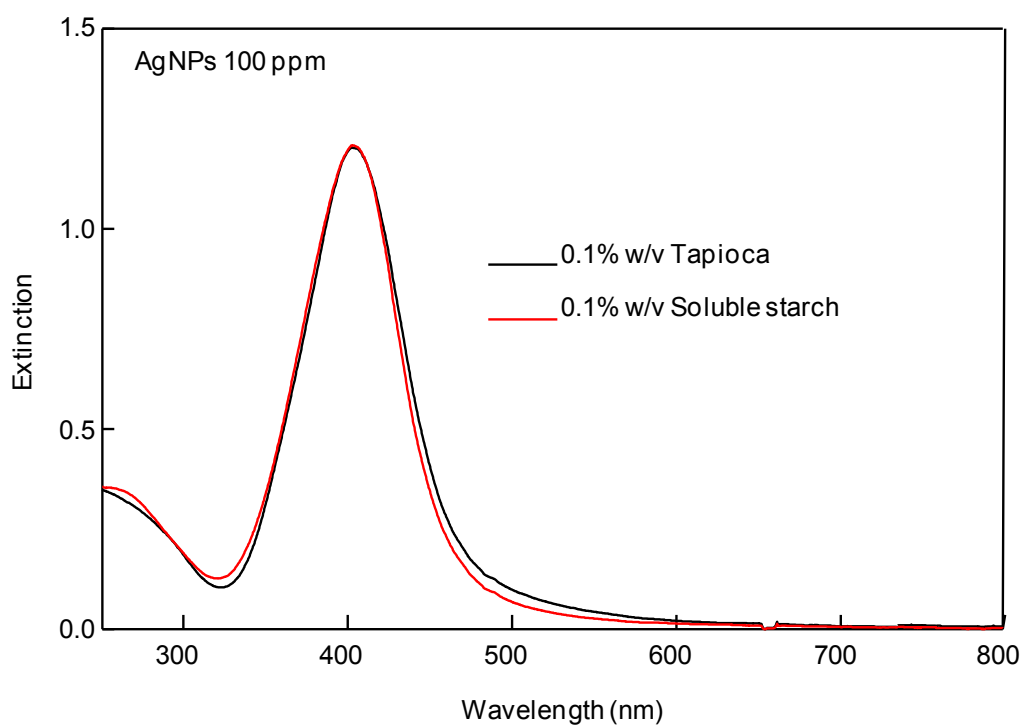
Figure 4.14 The plasmon extinction spectra of synthesized silver nanoparticles reduced with tapioca and soluble starch.

The extinction spectra of synthesized silver nanoparticles with 0.1% w/v tapioca and 0.1% w/v soluble starch displayed in Figure. 4.14 show a well-defined plasmon band at 400 nm.

4.8 Comparison of green synthesis method and sodium borohydride method

UV-visible extinction spectra of synthesized silver nanoparticles *via* green synthesis method and sodium borohydride method were measured. The results were compared to investigate the size and size distribution of silver nanoparticles.
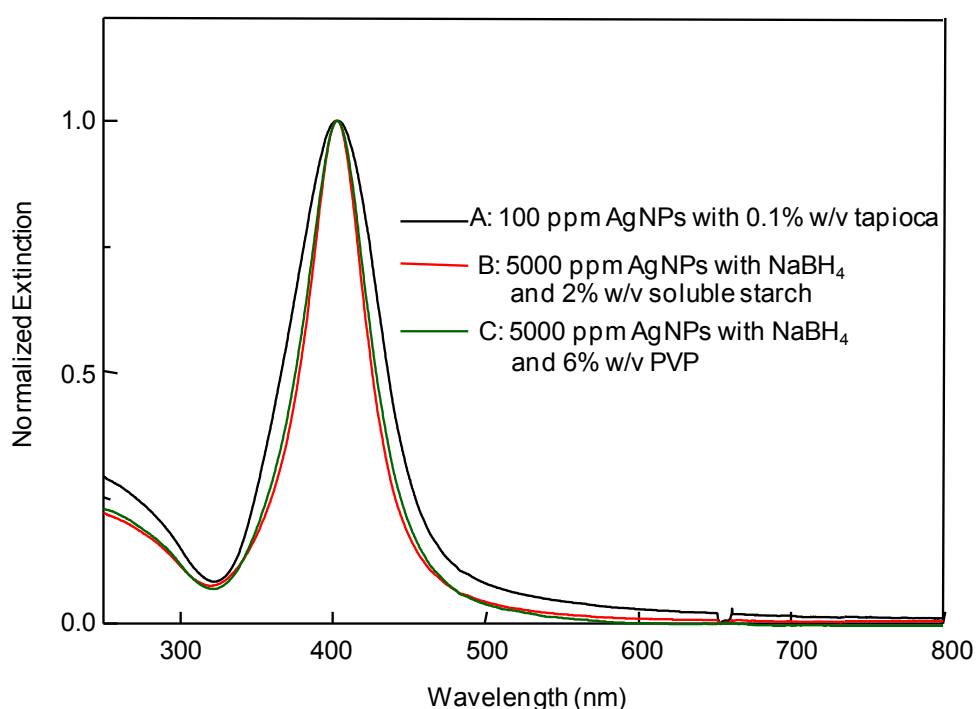
Figure 4.15 The normalized extinction spectra of synthesized silver nanoparticles *via*
green synthesis method (A) and sodium borohydride method (B-C).

The normalized extinction spectra of synthesized AgNPs *via* green synthesis method and sodium borohydride method are shown in Figure 4.15. The spectra show a well-defined plasmon band at 400 nm and there were slightly change in FWHM.

TEM images and histogram of synthesized AgNPs *via* green synthesis (A) and sodiumborohydride method (B-C) were shown in Figure 4.16. The synthesized AgNPs with sodium borohydride as a reducing agent, the particles are smaller than using tapioca. The average particles size of synthesized AgNPs via sodium borohydride method with 2% w/v soluble starch and 6% w/v polyvinylpyrrolidone are 10.46 ± 5.34 nm and 12.92 ± 3.85 nm, respectively.
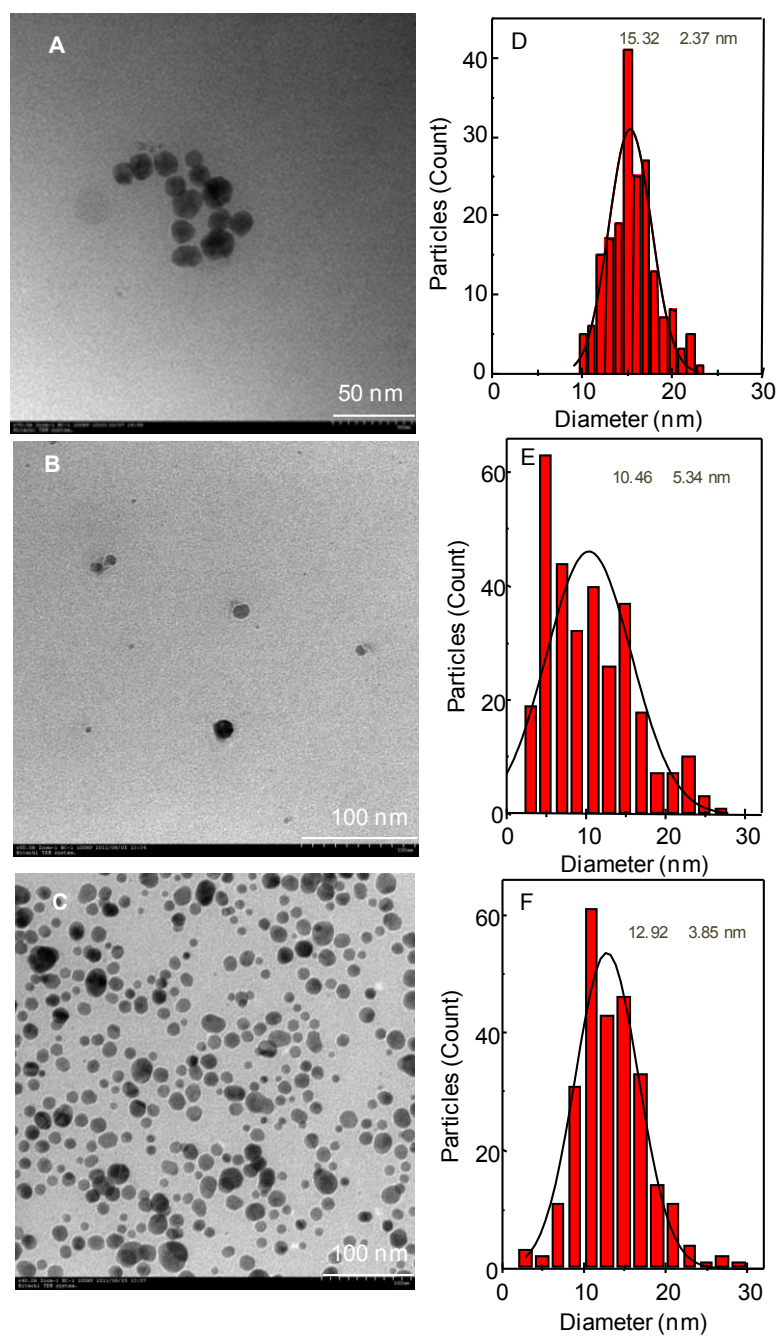
Figure 4.16 TEM images of synthesized silver nanoparticles *via* green synthesis (A) and sodium borohydride method (B-C). Histogram showing the particle size distribution of the synthesized silver nanoparticles *via* green synthesis (D) and sodium borohydride method (E-F).

4.9 Antibacterial activity of the synthesized silver nanoparticles

We investigated the antibacterial properties of synthesized silver nanoparticles against the Gram-negative bacterium *Escherichia coli (E. coli*) and Gram-positive bacterium *Staphylococcus aureus (S. aureus),* on agar plates containing different concentrations of nanoparticles. Tables 4.3 and 4.4 show percent reduction of bacteria as a function of the concentration of silver nanoparticles when approximately 10^6 CFU were applied to the plates.

Table 4.3 Antibacterial activities against *Escherichia coli* shown as percent reduction of bacteria

Sample	*Escherichia coli*		% reduction
	CFU/ml		
	0 h	24 h	
Control	2.25×10^6	8.75×10^5	61.11
AgNPs 2.5 ppm	2.25×10^6	$< 1.0 \times 10^1$	99.99
AgNPs 5 ppm	2.25×10^6	$< 1.0 \times 10^1$	99.99
AgNPs 10 ppm	2.25×10^6	$< 1.0 \times 10^1$	99.99

Table 4.4 Antibacterial activities against *Staphylococcus aureus* shown as percent reduction of bacteria

Sample	*Staphylococcus aureus*		% reduction
	CFU/ml		
	0 h	24 h	
Control	3.22×10^6	2.65×10^6	17.57
AgNPs 2.5 ppm	3.22×10^6	$< 1.0 \times 10^1$	99.99
AgNPs 5 ppm	3.22×10^6	$< 1.0 \times 10^1$	99.99
AgNPs 10 ppm	3.22×10^6	$< 1.0 \times 10^1$	99.99

This study shows that silver nanoparticles have excellent antibacterial activity against *E. coli.* and *S. aureus.* A very low concentration of silver nanoparticles (2.5 ppm) was shown to be an effective bactericide.

CHAPTER V

CONCLUSIONS

The present study demonstrates an eco-friendly and low cost protocol for synthesis of silver nanoparticles using tapioca solution supplied with aqueous silver (Ag^+) ions. Tapioca has been used both as reducing agent and stabilizer. 100 ppm of silver nanopartiles can be synthesized from tapioca after treated with acid hydrolysis and alkaline degradation.

The optimal condition for synthesizing AgNPs that are stable more than 2 months (no precipitation) were as follows: using 20 mL of 0.1M NaOH added into 0.1% tapioca solution and incubate solution at 80 °C for 40 min. Then the tapioca shows the efficiency to generate reducing species completely reduce silver ions and sufficiency stabilizes the obtained silver nanoparticles (AgNPs). Strong surface plasmon resonance peaks were observed at about 400 nm. The particles are spherical in shape with uniform distribution. The particle size ranged from 10 to 23 nm and histogram showed the particle size distribution of the synthesized silver nanoparticles with the average particles size 15.3 nm and standard deviation (σ) 2.4 nm. When the volume of NaOH was added more enough (excess base), the plasmon band was shifted to higher wavelength (red shift) about 570 nm; this means that shows there are some aggregrated particles and silver nanoplate. This might due to excess bases which decomposed the tapioca that acted as the stabilizing agent.

The correlation between reduction time and particles generation that tapioca treated with 20 mL of 0.1 M NaOH had enough reducing power to convert silver ions to silver particles and after 10 min, the reduction reaction are almost complete.

X-ray diffraction (XRD) showed that the silver nanoparticles were face centered cubic (fcc) structure. In order to investigate the effect of acidic-alkaline treatment on the degradation of tapioca; the solution was analyzed by attenuated total reflection Fourier transform infrared spectroscopy (ATR FT-IR). Some of the degradation intermediates contain functional groups with reduction potential (i.e.,

aldehyde and α-hydroxy ketone moieties). The observed spectral change agreed with the alkaline degradation of polysaccharide given by the Nef-Isbell mechanism.

The synthesized silver nanoparticles have excellent antibacterial activity against *E. coli.* and *S. aureus.* A very low concentration of silver nanoparticles (2.5 ppm) was shown to be an effective bactericide.

REFERENCES

[1] Mongillo, J. F. <u>Nanotechnology 101</u>, Greenwood Press: United State of America, 2007, 103-124.

[2] Gao, X., Wei, L., Wang, J., and Xu. B. Green synthesis of starch-stabilized silver nanoparticles and antibacterial properties. <u>Adv. Mat. Res.</u> 236 (2011): 1945-1948.

[3] Du, Z., and others. Green synthesis of silver nanoparticles using *Flos Sophorae Immaturus* extract and bactericidal activity. <u>Adv. Mat. Res.</u> 317 (2011): 475-478.

[4] Huang, N. M., and others. Sucrose ester micellar-mediated synthesis of Ag nanoparticles and the antibacterial properties. <u>Colloid Surface A</u> 353 (2010): 69-76.

[5] Panacek, A., and others. Silver colloid nanoparticles: synthesis, characterization and their antibacterial activity. <u>J. Phys. Chem. B</u> 110 (2006): 16248-16253.

[6] Ahamed, M., Khan, M. A. M., Siddiqui, M. K. J., Alsalhi, M. S., and Alrokayan, S. A. Green synthesis, characterization and evaluation of biocompatibility of silver nanoparticles. <u>Physica E</u> 43 (2011): 1266-1271.

[7] Moulton M. C., and others. Synthesis, characterization and biocompatibility of "green" synthesized silver nanoparticles using tea polyphenols. <u>Nanoscale</u> 2 (2010): 763-770.

[8] Vaidyanathan, R., Kalishwaralal, K., Gopalram, S., and Gurunathan, S. Nanosilver-the burgeoning therapeutic molecule and its green synthesis. <u>Biotechnol. Adv.</u> 27 (2009): 924-937.

[9] Tien, D.-C., Tseng, K.-H., Liao, C.-Y., and Tsung, T.-T. Colloidal silver fabrication using the spark discharge system and its antimicrobial effect on *Staphylococcus aureus*. <u>Med. Eng. Phys.</u> 30 (2008): 948-952.

[10] Turker M. Effect of production parameters on the structure and morphology of Ag nanopowders produced by inert gas condensation. <u>Mater. Sci. Eng. A</u> 367 (2004): 74-81.

[11] Mafune F.; Kohno J.; Takeda, Y.; Kondow T. Structure and stability of silver nanoparticles in aqueous solution produced by laser ablation. <u>J. Phys. Chem. B</u> 104 (2000): 8333-8337.

[12] Pluym T. C. et al. Solid silver particle production by spray pyrolysis. <u>J. Aerosol Sci.</u> 24 (1993): 383-392.

[13] Shi, X., Wang, S., Duan, X., and Zhang, Q. Synthesis of nano Ag powder by template and spray pyrolysis technology. <u>Mater. Chem. Phys.</u> 11 (2008): 1110-1113.

[14] Kassaee, M.Z., Akhavan, A., Sheikh, N., and Beteshobabrud, R. γ-Ray synthesis of starch-stabilized silver nanoparticles. <u>Radiat. Phys. Chem.</u> 77 (2008): 1074-1078.

[15] Lee, S.H., Oh, S.M., and Park, D.W. Preparation of silver nanopowder by thermal plasma. <u>Mater. Sci. Eng. C</u> 27 (2007): 1286-1290.

[16] Hu, Y., Ge, J., Lim, D., Zhang, T., and Yin, Y. Size-controlled synthesis of highly water-soluble silver nanocrystals. <u>J. Solid State Chem.</u> 181 (2008): 1524-1529.

[17] Can-Amares M. V., Garcia-Ramos J. V., and Gomez-Varga J. D. Comparative study of the morphology, aggregation, adherence to glass, and surface-enhanced Raman scattering activity of silver nanoparticles prepared by chemical reduction of Ag+ using citrate and hydroxylamine. <u>Langmuir</u> 21 (2005): 8546-8553.

[18] Henglein, A., and Giersig, M. Formation of colloidal silver nanoparticles: capping action of citrate. <u>J. Phys. Chem. B</u> 103 (1999): 9533-9539.

[19] Wang, H., Qiao, X., Chen, J., and Ding, S. Preparation of silver nanoparticles by chemical reduction method. <u>Colloid Surface A</u> 256 (2005): 111-115.

[20] Huang, H. H. and others. Photochemical formation of silver nanoparticles in Poly (N-vinylpyrrolidone). <u>Langmuir</u> 12 (1996): 909-912.

[21] Zhang, Z., Patel, R. C., Kothari, R., Johnson, C. P., and Friberg, S. E. Stable silver clusters and nanoparticles prepared in polyacrylate and inverse micellar solutions. J. Phys. Chem. B 104(2000): 1176-1182.

[22] Filippo, E., Serra, A., and Manno, D. Poly (vinyl alcohol) capped silver nanoparticles as localized surface plasmon resonance-based hydrogen peroxide sensor. Sensor Actuat B-Chem 138 (2009): 625-630.

[23] Dahl, J.A., Maddux, B. L. S., Stievano, L., and Hutchison, J.E. Toward greener nanosynthesis. Chem. Rev. 107 (2007): 2228–2269.

[24] Sharma, V.K., Yngard, R.A., and Lin, Y. Silver nanoparticles: green synthesis and their antimicrobial activities. Adv. Colloid Interfac. 145 (2009): 83-96.

[25] Hu, B., Wang, S., Wang, K., Zhang, M., and Yu, S. Microwave-assisted rapid facile "green" synthesis of uniform silver nanoparticles: self assembly into multilayered films and their optical properties. J. Phys. Chem. C 112 (2008): 11169-11174.

[26] Raveendran, P., Fu, J., and Wallen, S.L. Completely green synthesis and stabilization of metal nanoparticles. J. Am. Chem. Soc. 125 (2003): 13940-13941.

[27] Vigneshwaran, N., Nachane, R. P., Balasubramanya R. H., and Varadarajan, P. V. A novel one-pot „green" synthesis of stable silver nanoparticles using soluble starch. Carbohyd. Res. 341 (2006): 2012-2018.

[28] Manno, D., Filippo, E., Giulio, M. D., and Serra, A. Synthesis and characterization of starch-stabilized Ag nanostructures for sensors applications. J. Non-Cryst. Solids. 354 (2008): 5515-5520.

[29] Dubas, S. T., and Pimpan, V. Green synthesis of silver nanoparticles for ammonia sensing. Talanta 76 (2008): 29-33.

[30] Bar, H., Bhui, D. Kr., Sahoo, G.P., Sarkar, P., De, S.P., and Misra, A. Green synthesis of silver nanoparticles using latex of *Jatopha curcas*. Colloid Surface A 339 (2009): 134-139.

[31] Khanna, P.K., and Nair, C. K. K. Synthesis of silver nanoparticles using cod liver oils (fish oil): green approach to nanotechnology. Int. J. Green Nanotech. 1 (2009): 3-9.

[32] Bankar, A., Joshi, B., Kumar, A. R., and Zinjarde, S. Banana peel extract mediated novel route for the synthesis of silver nanoparticles. <u>Colloid Surface A</u> 368 (2010): 58-63.

[33] Filippo, E., Serra, A., Buccolieri, A., and Manno, D. Green synthesis of silver nanoparticles with sucrose and maltose: Morphological and structural characterization. <u>J. Non-Cryst. Solids.</u> 336 (2010): 344-350.

[34] Li, S., and others. Green synthesis of silver nanoparticles using *Capsicum annuum* L. extract. <u>Green Chem.</u> 9 (2007): 852-858.

[35] Song, J. Y., and Kim, B. S. Rapid biological synthesis of silver nanoparticles using plant leaf extracts. <u>Bioproc. Biosyst. Eng</u>. 32 (2009): 79-84.

[36] Phillip, D. Honey mediated green synthesis of silver nanoparticles. <u>Spectrochim. Acta A</u> 75 (2010): 1078-1081.

[37] Dubey, S. P., Lahtinen, M., and Sillanpaa, M. Tansy fruit mediated greener synthesis of silver and gold nanoparticles. <u>Proc. Biochem.</u> 45 (2010): 1065-1071.

[38] Jha, A. K., and Prasad, K. Green synthesis of silver nanoparticles using *Cyas* Leaf. <u>Int. J. Green Nanotech: Phys. and Chem.</u> 1 (2010): 110-117.

[39] Njagi, E. C., and others. Biosynthesis of iron and silver nanoparticles at room temperature using aqueous sorghum bran extracts. <u>Langmuir</u> 27 (2011): 264-271.

[40] Philip, D., Unni, C., Aromal, S. A., and Vidhu, V. K. Murraya Koenigii leaf-assisted rapid green synthesis of silver and gold nanoparticles. <u>Spectrochim. Acta A</u> 78 (2011): 899-904.

[41] Jain, N., Bhargava, A., Majumdar, S., Tarafdar, J. C., and Panwar, J. Extracellular biosynthesis and characterization of silver nanoparticles using *Aspergillus flavus* NJP08: A mechanism perspective. <u>Nanoscale</u> 75 (2010): 1078-1081.

[42] Ramirez, M. G. L., Muniz, G. I. B., Satyanarayana, K. G., Tanobe, V., and Iwakiri, S. Preparation and characterization of biodegradable composites based on Brazilian cassava starch, corn starch and green coconut fibers. <u>Rev. Mater.</u> 15 (2010): 330-337.

[43] Swinkels, J. J. M. Composition and properties of commercial native starches. Starch-Starke 37 (1985): 1-5.

[44] Sajilat, M. G., Singhal, R. S., and Kulkarni P. R. Resistant starch-review. Compr. Rev. Food Sci. F. 5 (2006): 1-17.

[45] Kelsall, R., Hamley, I., and Geoghegan, M. Nanoscale Science & Technology. Japan: Wiley, 2005.

[46] Kelly, K. L.; Coronado E.; Zhao L. L.; Schatz G. C. The optical properties of metal nanoparticles: the influence of size, shape, and dielectric environment. J. Phys. Chem. B 107 (2003): 668-677.

[47] Wiley, B. J., and others. Maneuvering the surface plasmon resonance of silver nanostructures through shape-controlled synthesis. J. Phys. Chem. B 110 (2006): 15666-15675.

[48] Pillai Z. S.; Kamat P.V. What factors control the size and shape of silver nanoparticles in the citrate ion reduction method? J. Phys. Chem. B 108 (2004): 945-951.

[49] Sondi, I., and Salopek-Sondi B. Silver nanoparticles as antimicrobial agent: a case study on *E. coli* as a model for Gram-negative bacteria. J. Colloid Interf. Sc. 275 (2004): 177-182.

[50] Wong, K. K. Y., and Liu, X. Silver nanoparticles- the real "silver bullet" in clinical medicine? Med. Chem. Commun., 1 (2010): 125-131.

[51] Chaloupka, K., Malam Y., and Seifalian A. M. Nanosilver as a new generation of nanoproduct in biomedical applications. Trends Biotechnol. 28 (2010): 580-588.

[52] Rai, M., Yadav, A., and Gade, A. Silver nanoparticles as a new generation of antimicrobials. Biotechnol. Adv. 27 (2009): 76–83.

[53] Marambio-Jones, C., and Hoek, E. M. V. A review of the antibacterial effects of silver nanomaterials and potential implications for human health and the environment. J. Nanopart. Res. 12 (2010): 1531-1551.

[54] Chao, J. B., and others. Speciation analysis of silver nanoparticles and silver ions in antibacterial products and environmental waters via cloud point extraction-based separation. Anal. Chem. 83 (2011): 6875-6842.

[55] Wei, D., Sun, W., Qian, W., Ye, Y., and Ma, X. The synthesis of chitosan-based silver nanoparticles and their antibacterial activity. <u>Carbohyd. Res.</u> 344 (2009): 2375-2382.

[56] Li, W. R., Xie, X. B., Shi, Q. S., Zeng, H., Ou-Yang, Y. S., and Chen, Y. B. Antibacterial activity and mechanism of silver nanoparticles on *Escherichia coli*. <u>Appl. Microbiol. Biotechnol.</u> 85 (2010): 1115-1122.

[57] Pal, S., Tak, Y. K., and Song, J. M. Does the antibacterial activity of silver nanoparticles depend on the shape of the nanoparticle? A study of the gram-negative bacterium *Escherichia coli*. <u>Appl. Environ. Microbiol.</u> 73 (2007): 1712-1720.

[58] Choi, O., and Hu, Z. Size dependent and reactive oxygen species related nanosilver toxicity to nitrifying bacteria. <u>Environ. Sci. Technol.</u> 42 (2008): 4583-4588.

[59] Johnston, H. J., Hutchison, G., Christensen, F. M., Peter, S., Hankin, S., and Stone, V. A review of the in vivo and in vitro toxicity of silver and gold particulates: particle attributes and biological mechanisms responsible for the observed toxicity. <u>Crit. Rev. Toxicol.</u> 40 (2010): 328-346.

[60] Liu, W., and others. Impact of silver nanoparticles on human cells: effect of particle size. <u>Nanotoxicology</u> 4 (2010): 319-330.

[61] Yu, C.-H, Tam, K., and Tsang, E. S. C. <u>Handbook of metal physics</u>, Elsevier B. V., 2009.

[62] Kizil, R., Irudayaraj, J., and Seetharaman, K. Characterization of irradiated starches by using FT-Raman and FTIR spectroscopy. <u>J. Agric. Food Chem.</u> 50 (2002): 3912-3918.

[63] Betancourt, A. N. D., and Chel G. L <u>J. Agric. Food Chem.</u> 45 (1997): 4237-4241.

[64] Socrates, G. <u>Infrared and Raman Characteristic Group Frequencies: Tables and Charts</u>, 3rd ed.; John Wiley & Sons Ltd: Chichester, U. K., 2001.

[65] Reintjes, M., and Cooper, G. K. Polysaccharide alkaline degradation product as a source of organic chemical, <u>Ind. Eng. Chem. Prod. Res. Dev.</u> 23 (1984): 70–73.

[66] Knill, C. J., and Kennedy, J. F. Degradation of cellulose under alkaline conditions. Carbohyd. Polym. 51 (2003): 281-300.

[67] Clarke, M. A., Edye, L. A., and Eggleston, G. Advances in carbohydrate chemistry and biochemistry, Academic Press 1997; Vol. 52, 449–455.

[68] Sinnott, M. L. Carbohydrate Chemistry and Biochemistry, The Royal Society of Chemistry 2007, 492–497.

[69] Coated, J. Encyclopedial of Analytical Chemistry, John Wiley & Sons Ltd, Chichester, USA, 2000, 10815–10837.

[70] Venkatpurwar, V., and Pokharkar, V. Green synthesis of silver nanoparticles using marine polysaccharide: study of in-vitro antibacterial activity. Mater. Lett. 65 (2011): 999-1002.

APPENDIX

I : keto-enol tautomerism

			H-O-H		

HC=O
H–C–OH
HO–CH
HC–O Glu n
HC–OH
CH₂OH

HO OH

HC=O
H–C–OH
HO–CH
HC–O Glu n
HC–OH
CH₂OH

HC–O
C–OH
HO–CH
HC–O Glu n
HC–OH
CH₂OH

HC–OH
C–OH
HO–CH
HC–O Glu n
HC–OH
CH₂OH

II : enediol deprotonation

HC–OH
C–OH
HO–CH
HC–O Glu n
HC–OH
CH₂OH

OH

HC–O–H OH
C–OH
HO–CH
HC–O Glu n
HC–OH
CH₂OH

HC–O
C–OH
HO–CH
HC–O Glu n
HC–OH
CH₂OH

III : anion isomerisation

HC–OH
C–OH
HO–CH
HC–O Glu n
HC–OH
CH₂OH

OH

HC–O–H OH
C–OH
HO–CH
HC–O Glu n
HC–OH
CH₂OH

HC–O
C–O–H
HO–CH
HC–O Glu n
HC–OH
CH₂OH

HC–OH
C–O
HO–CH
HC–O Glu n
HC–OH
CH₂OH

IV : β-hydroxycarbonyl elimination

HC–O
C–OH
HO–CH
HC–O Glu n
HC–OH
CH₂OH

HC–O
C–OH
HO–CH
HC–O(Glu)n
HC–OH
CH₂OH

- OH

HC=O
C–OH
CH
HC–O(Glu)n
HC–OH
CH₂OH

V : β-alkoxycarbonyl elimination   H–O–H

HC–OH
C–O
HO–CH
HC–O Glu n
HC–OH
CH₂OH

(V)

HC–OH
C–O
HO–C–H
HC–O Glu n
HC–OH
CH₂OH

CH₂OH
C=O
C–OH
C–H
HC–OH
CH₂OH

Scheme 1. Reaction mechanism of starch under alkaline degradation.

I : β-elimination
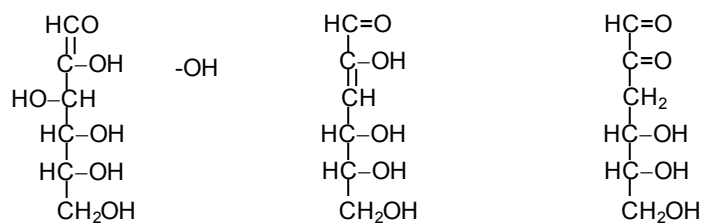
```
HCO                  HC=O                 HC=O
 ‖                    ‖                    ‖
 C–OH    -OH          C–OH                 C=O
HO–CH                 CH                   CH₂
HC–OH                 HC–OH                HC–OH
HC–OH                 HC–OH                HC–OH
CH₂OH                 CH₂OH                CH₂OH
```

II : benzilic acid rearrangement

```
                     OH                   OH                   O
HC=O                 H–C–O                C=O                  C=O
C=O      OH          C=O                  H–C–O                H–C–OH
CH₂                  CH₂                  CH₂                  CH₂
HC–OH                HC–OH                HC–OH                HC–OH
HC–OH                HC–OH                HC–OH                HC–OH
CH₂OH                CH₂OH                CH₂OH                CH₂OH
```

III : α-dicarbonyl clevage

```
                     OH                   HCOOH
HC=O                 H–C–O
C=O      OH          C=O                  +
CH₂                  CH₂                  HC=O
HC–OH                HC–OH                CH₂
HC–OH                HC–OH                HC–OH
CH₂OH                CH₂OH                HC–OH
                                          CH₂OH
```

IV : retro-aldolization

```
                     H–C–OH
HC–OH                C–OH
 ‖                    ‖
C–OH     OH          HO–C–H
HO–C–H               +
HC–O–H               H–C=O
HC–OH                H–C–OH
CH₂OH                 ‖
                     H–CH₂OH
```

IV : aldolization

```
                                          H–C=O
H–C–O        H–C=O        H–C=O           H–C–OH
 ‖                        +                H–C–O
H–C–OH       H–C–OH           H
                                          H
```
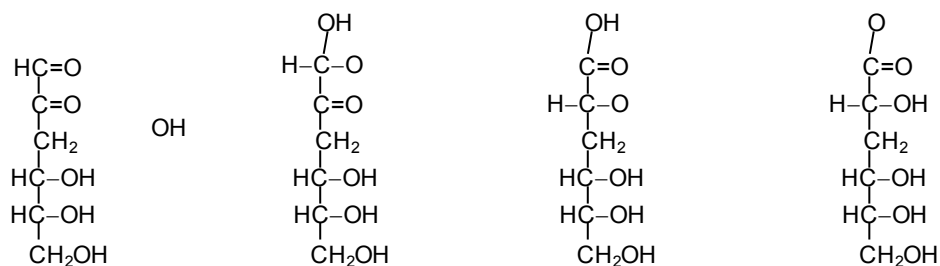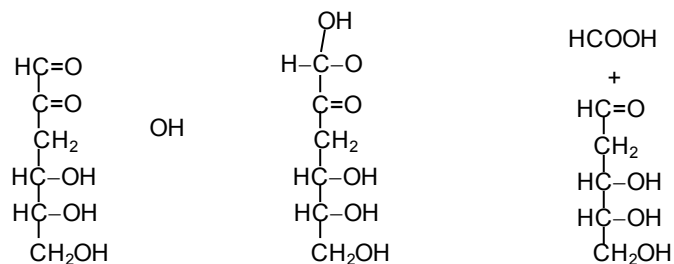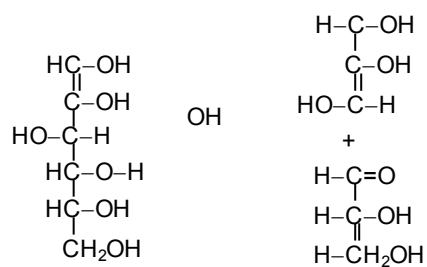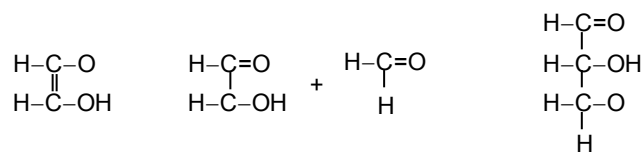
Scheme 2. Reaction mechanism of monosaccharide under alkaline degradation.

VITAE

Name: Miss Wimonnan Sroisuriya

Date of Birth: May 8, 1974   **Birth place:** Phitsanulok, Thailand

Address: 337/7, Sriharajdechochai road, Amphur Mueang, Phitsanulok

65000, Thailand, E-mail address: wimonnan@gmail.com

Education:

1995	Bachelor of Science in Chemistry, Chiang Mai University
2001	Master of Science in Chemistry, Chiang Mai University
2011	Doctor of Philosophy in Chemistry, Chulalongkorn University

Work place: Chemistry Program, Faculty of Science and Technology, Loei Rajabhat University, Loei

Conferences:

November 1, 2008	34th Congress on Science and Technology of Thailand
March 12-13, 2009	The Science Forum 2009, Thailand
August 27-29, 2009	Commission on Higher Education Congress II University Staff Development Consortium (CHE-USDC Congress II), Thailand
October 26-28, 2010	36th Congress on Science and Technology of Thailand
January 5-7, 2011	The 28th Annual Conference of The Microscopy Society of Thailand
March 10-11, 2011	The Science Forum 2011, Thailand
March 24-25, 2011	The Second International Conference on Applied Science (2nd ICAS), LAO People's Democratic Republic

Awards:

March 12-13, 2009	The Third award in Oral presentation in The Science Forum 2009, Thailand
March 10-11, 2011	The Second award in Oral presentation in The Science Forum 2011, Thailand